Construction of tectonic subsidence curves for the early Paleozoic miogeocline, southern Canadian Rocky Mountains: Implications for subsidence mechanisms, age of breakup, and crustal thinning

GERARD C. BOND
MICHELLE A. KOMINZ
Lamont-Doherty Geological Observatory of Columbia University, Palisades, New York 10964

ABSTRACT

A quantitative procedure has been developed for calculating tectonic subsidence in fully lithified strata and has been applied to stratigraphic sections in the early Paleozoic miogeocline of the southern Canadian Rocky Mountains. The results indicate that tectonic subsidence along the inner edge of the miogeocline was controlled mainly by thermal contraction of heated lithosphere. Comparison of a palinspastically restored cross section of the inner part of the miogeocline with a cross section constructed from a two-dimensional stretching model suggests that thinned continental crust was present beneath the inner miogeocline. These results support the passive-margin model that has been proposed for the miogeocline. The extensive transgression onto the craton east of the miogeocline in Cambrian time, however, cannot be explained by subsidence processes operating within a passive margin, and the transgression could be evidence for a eustatic rise of sea level.

The form of the tectonic subsidence curves strongly implies that cooling of the heated lithosphere, which was initiated at the time of breakup, could not have begun earlier than the latest Precambrian or earliest Cambrian (555 Ma to 600 Ma). Ages of 800 Ma to 900 Ma that have been assumed previously for rifting in the miogeocline are too old to have led directly to continental breakup. Scattered occurrences of mafic volcanics interlayered with arkosic sediments have been reported in the latest Precambrian to earliest Cambrian Hamill Group exposed in the middle to outer part of the miogeocline. These deposits may record the phase of rifting that immediately preceded formation of the proto-Pacific margin in the southern Canadian Rockies.

INTRODUCTION

The presence of an early Paleozoic miogeocline in the North American Cordillera was interpreted by Stewart (1971, 1972) and by Burchfiel and Davis (1972) as evidence that a passive continental margin was initiated at some time in the late Precambrian along the western edge of the North American craton. This interpretation was based on a comparison of the geology of the miogeocline with the generalized and largely descriptive models of passive margins that were available at the time.

In recent years, new quantitative methods and geophysical models have been developed for analyzing the evolution of modern passive margins (Keen, 1982; Watts, 1981). In this paper, the evolution of a part of the Cordilleran miogeocline in the southern Canadian Rocky Mountains is re-examined using a quantitative method for analyzing subsidence that has been applied recently to modern passive margins. This method involves the construction of tectonic subsidence curves from columnar stratigraphic sections (Sleep, 1971; Watts and Ryan, 1976). Tectonic subsidence, which is subsidence caused solely by a tectonic or driving mechanism, is calculated by quantitatively removing the subsidence produced by nontectonic processes such as sediment loading, sediment compaction, and water depth changes. The advantage of this procedure is that a graph of tectonic subsidence versus time, the tectonic subsidence curve, can be compared with subsidence curves calculated from various geophysical models of passive margins. The comparison of such curves has been found to be especially useful as a means of identifying the thermal component of subsidence and its timing in the postrift cooling stages of modern passive margins (Sleep, 1971; Keen, 1979; Watts and Steckler, 1979).

This paper begins with the development of a new method that has been briefly described previously (Bond and Kominz, 1981; Kominz and Bond, 1982) for recovering the tectonic component of subsidence from fully lithified and lithologically diverse strata of the type that are typically present in the Cordilleran miogeocline. We apply this method to selected stratigraphic sections in the thrust and fold belt of the southern Canadian Rockies, where the strata are exceptionally well exposed and good stratigraphic and structural controls have been established. The results of the analysis are compared with thermal-mechanical models of passive margins to identify the mechanisms that controlled the subsidence and to obtain a new estimate for the age of continental breakup and initiation of the passive margin in the southern Canadian Rockies

PROCEDURE FOR CALCULATING TECTONIC SUBSIDENCE IN THE MIOGEOCLINAL STRATA

The procedure we use to calculate tectonic subsidence in the miogeoclinal strata is a modification of the backstripping method that was originally developed by Sleep (1971) and later applied to the northwestern Atlantic margin by Watts and Ryan (1976) (see Steckler and Watts, 1978; and Sclater and Christie, 1980, for detailed discussion of the method). The procedure, shown diagrammatically in Figure 1, begins by restoring the lowest unit in a stratigraphic section, usually a formation or member, to its initial thickness and bulk density (unit 1a in Fig. 1) and placing its top at a depth below sea level corresponding to the average depth of water in which the unit was deposited (Wd_1). The isostatic subsidence of the basement caused by the weight of the sediment in the unit is then removed, and the depth to the surface on which the unit was deposited (Y_1) is recalculated with only the weight of water as the basement loading factor. Next, the second unit in the section is restored to its initial thickness and bulk density (unit 2a) and is positioned with its top at the average depth of deposition of the unit (Wd_2) and its base in contact with the first unit. The thickness and bulk density of the first unit are adjusted (unit 1b) in accordance with the depth of burial beneath the second unit. The isostatic subsidence due to the weight of sediment in both

Geological Society of America Bulletin, v. 95, p. 155–173, 11 figs., 1 table, February 1984.

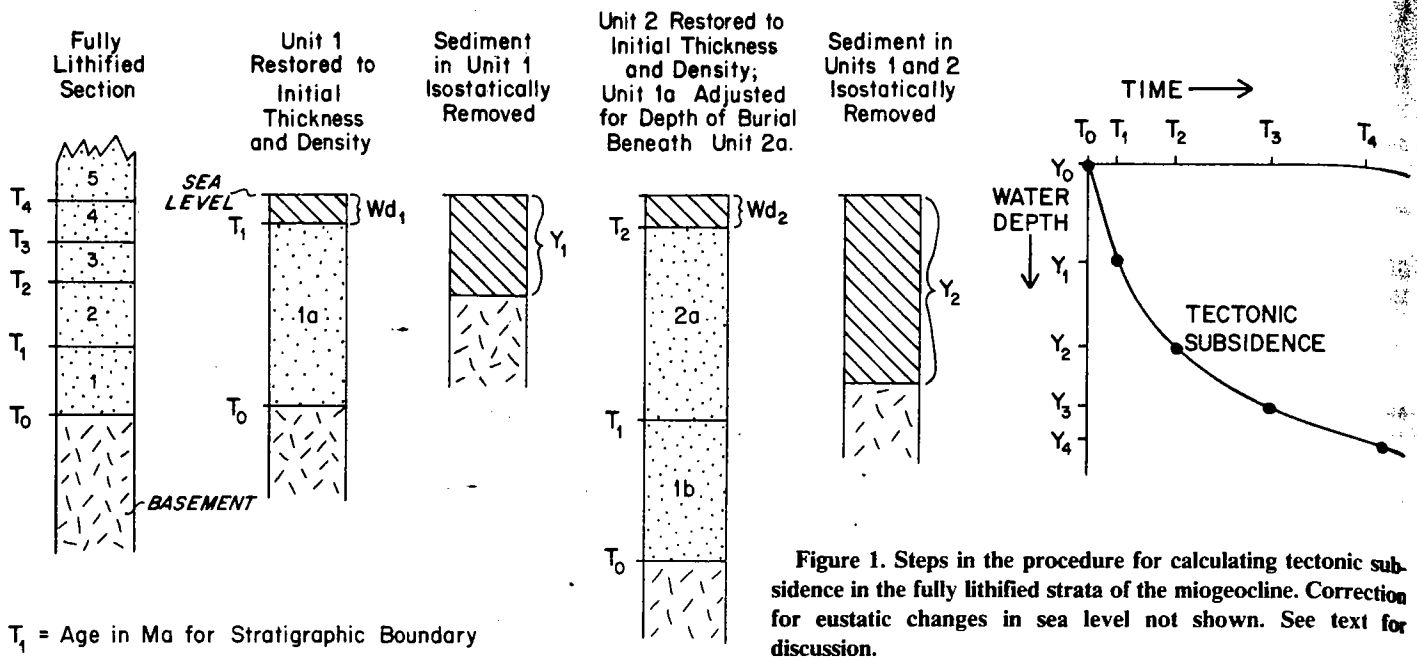

Figure 1. Steps in the procedure for calculating tectonic subsidence in the fully lithified strata of the miogeocline. Correction for eustatic changes in sea level not shown. See text for discussion.

the first and second units is removed as before, and the depth to the surface on which the first unit was deposited (Y_2) is again recalculated with only the weight of water as the loading factor. These steps are repeated for successively higher units until they are completed for the highest unit in the section. To complete the procedure, the water depths should be corrected for any eustatic changes in sea level, if known, using the method described by Steckler and Watts (1978) (this step not shown in Fig. 1). The tectonic subsidence curve for the section is given by plotting the values of Y as a function of radiometric ages of the stratigraphic units (Fig. 1). If the base of unit 1 was not deposited close to sea level, the first point on the tectonic subsidence curve (Y_0) must be plotted at the water depth for the base of that unit.

Calculation of Tectonic Subsidence

The calculation of tectonic subsidence in a unit of a stratigraphic section is given by the general equation that has been developed for modern sedimentary basins (Steckler and Watts, 1978):

$$Y = \Phi\left[S^*\left(\frac{\rho_m-\rho_s}{\rho_m-\rho_w}\right) - \Delta SL\left(\frac{\rho_w}{\rho_m-\rho_w}\right)\right] + \left[Wd - \Delta SL\right] \quad (1)$$

where Y = tectonic subsidence, S* = sediment thickness corrected for compaction, ρ_s = mean bulk density of sediments, ρ_m = mean density of mantle (3.40 g/cm^3), ρ_w = density of sea water, ΔSL = change in sea level relative to its present-day elevation, Φ = a basement response or weighting function relating sediment and water loads to tectonic subsidence, and Wd = average depth of water in which unit was deposited.

This equation is not directly applicable to the miogeoclinal sequences, however, because of the way in which S*, the decompacted sediment thickness, has been calculated. For modern basins, calculation of S* has been simplified by assuming that thicknesses and porosities of the sedimentary layers decrease during burial solely by compaction resulting from mechanical processes and/or pressure solution with precipitation of all dissolved material in pore space (Van Hinte, 1978; Perrier and Quiblier, 1974; Steckler and Watts, 1978; Sclater and Christie, 1980). The change in thickness and density of a layer during burial, therefore, is assumed to be directly proportional to the decrease in porosity in that layer with depth. The decrease in porosity with depth is calculated using well-log data from drill holes in the margin. The change in porosity with depth cannot be determined in this manner for the sedimentary rocks in the miogeocline because their long exposure to diagenesis has reduced the porosities to essentially zero. Moreover, it is clear that compaction was not the only process that reduced porosities in the miogeoclinal strata. We have found from thin-section studies that in portions of certain lithologies, especially quartz sandstone and calcarenite with little matrix, the grains are loosely packed and the pore space is filled with cement. Such textures, which are widely recognized in both modern and ancient sediments, are evidence that porosities were reduced and the sediment lithified by precipitation of cements before the layers were buried deeply enough to be compacted (Beales, 1971; Bathurst, 1976; Choquette and Pray, 1970; Friedman, 1975). In other lithologies in the miogeocline, however, compaction appears to have been important, especially in shales and fine-grained limestones containing fluid escape structures and flattened burrows. To calculate S* for the miogeoclinal strata, therefore, the sedimentary layers must be delithified; that is, corrections must be made for both compaction and cementation during burial, and these corrections must be developed without direct porosity measurements as a guide.

A Procedure for Delithifying the Miogeoclinal Strata

The quantitative relations between depth of burial, compaction, and cementation are poorly understood, and it is not possible to specify a precise empirical or theoretical delithification factor for each lithology in the miogeocline. Quantitative delithification factors cannot be obtained directly from petrologic studies of the miogeoclinal sediments, either, because of the long and complex diagenetic processes that have affected them. It seems, therefore, that the best approach to delithification is to determine the maximum and minimum limits of the effects of compaction and cementation during burial of the strata and to assume that the ranges between the limits contain the correct values for delithification. We have found that this procedure can be developed readily from data in the literature and that the ranges between reasonable maximum and minimum limits are not unacceptably large.

The maximum limit for delithification is derived from the assumption that the thicknesses

and densities of each stratigraphic unit were changed during burial solely by compaction. To calculate this limit, it is necessary to determine the average initial porosity and the change in average porosity during burial of each stratigraphic unit. This is done using an empirical porosity versus depth curve for each of the most common lithologies in the stratigraphic units, which are micrite, calcisiltite, calcarenite, noncalcareous shale, quartz siltstone, and well-sorted quartz sandstone with little to no matrix (Fig. 2, solid curves). The construction of these curves is treated in the next section of the discussion. To calculate the initial average porosity, the stratigraphic unit is placed on the porosity curves with its top at zero depth and its base at the depth equivalent to its present thickness. The porosity curves corresponding to each lithology that is present in the unit are integrated from zero depth to the base of the unit and divided by the thickness of the unit. The average initial porosity is given by multiplying each result of this division by the percentage of the corresponding lithology in the unit and summing the products. The thickness of the unit is then increased by the amount of water needed to fill the initial average porosity. Because the addition of the water carries the base of the unit to a deeper level on the porosity curves, the steps for calculating the initial average porosity must be repeated using the new depth to the base of the unit. This procedure is repeated until the difference in successive values for average initial porosity is less than 2%. The initial thickness of the unit is calculated by adding its measured thickness to the thickness of water required to fill the pore space given by the last iteration for the average initial porosity. The average initial density of the unit is easily calculated from the average grain density of the unit and its average initial porosity. The average grain density is determined using densities for various nonporous lithologies given by Daly and others (1966) and the percentage of the lithologies in each unit. To obtain the change in thickness and average density of the unit with burial, thickness and average porosity are calculated as above but using the successively deeper segments of the porosity curves that correspond to the increasing depths of burial of the unit as successively younger units are placed above it. This procedure for calculating the maximum limit of delithification is valid for compaction caused by purely mechanical movement of grains closer together, by solution of the grains and reprecipitation of all dissolved material in nearby pore space, or by a combination of these two mechanisms.

The minimum limit for delithification is derived from the assumptions that only noncalcareous shales were compacted during burial and that the average initial porosities of all other lithologies were reduced solely by addition of cement. We specify that the cement originated in an external source and not from solution of grains within the section. The calculation of average initial porosity and change in porosity with burial is the same as for the maximum limit, with two exceptions. The porosity curves used for the calculation are the dashed curves in Figure 2, and the present or measured thicknesses of each unit are increased only by the amount of water required to fill the porosity in the fraction of noncalcareous shale in the unit. The density of the cement that is added to fill the pore space is set equal to the average grain density; therefore, the calculation of the increase in density with burial is the same as for the maximum limit. It should be clear that during progressive burial of each stratigraphic unit, the increase in density of all lithologies except noncalcareous shale is due entirely to addition of cement, and the thicknesses of all lithologies except noncalcareous shale remain equal to their measured or present-day thicknesses.

We recognize that elimination of porosity entirely by precipitation of a cement derived from an external source, as assumed for the minimum limit, is highly unlikely in a thick sedimentary sequence, in view of the extremely large volume of dissolved material that must be carried into the sedimentary column (Blatt, 1979; Bathurst, 1976). Even so, we choose to define the minimum limit in terms of an externally derived cement because it establishes a probable boundary on the range of lithification processes in sediments.

We have assumed in the procedures for delithification that the processes of compaction and cementation are mainly depth dependent rather than time dependent during progressive burial of sediment in a subsiding basin. Where the sedimentary layers are buried relatively rapidly, as in the miogeocline, this assumption is probably valid enough for our purposes. In addition, Schmoker and Halley (1982) suggested from their detailed study of carbonate porosities of south Florida that porosity reduction there was mainly a depth-dependent process.

The equations for calculating the maximum and minimum limits and the calculation of S* in terms of these limits are given in Appendix 1.

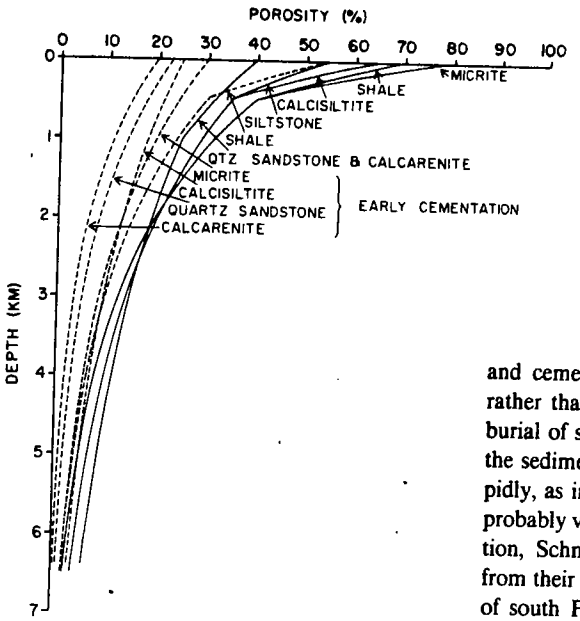

Figure 2. Empirical porosity-depth curves used for delithifying the miogeoclinal sequences. Solid curves are for maximum values of delithification, and dashed curves are for minimum values of delithification. Construction of the curves is described in the text.

Construction of Empirical Porosity Curves

The porosity curves in Figure 2 were constructed using general concepts of sediment diagenesis during burial and values for porosities as a function of depth in modern sedimentary deposits. The choice of exact values for the porosities was necessarily somewhat arbitrary, but the rate of change in the porosities with depth and the ranges between values for coarse- and fine-grained sediments are in accord with the available data.

The values for the surface porosities in the maximum and minimum curves are taken from the upper and lower limits, respectively, of ranges reported for typical surface porosities in coarse- to fine-grained limestones, clean quartz sandstones, siltstones, and noncalcareous shales in modern depositional environments (Enos and Sawatsky, 1980; Füchtbauer, 1974; Shinn and others, 1977; Coogan, 1970; Maxwell, 1964; Scholle, 1977; Von Engelhardt, 1973; Chilingarian and Wolf, 1975, 1976; Rieke and Chilingarian, 1974; Magara, 1980; Beard and Wyel, 1973). We do not assign a surface porosity of 0% to any sediment undergoing cementation because even hardgrounds, where exceptionally early cementation occurs, typically have more than 10% porosity near the surface (Scholle, 1977; Shinn, 1969). The curves for decrease of the surface porosities with depth are exponential in form for both the maximum and minimum limits. For the maximum limits (solid curves in Fig. 2), the porosity is reduced in two exponen-

tial segments, the upper of which has a faster rate of decay than does the lower. This form of the curves for the maximum limits is based on theoretical and empirical studies of sediment compaction that indicate that porosity reduction typically is exponential with increasing depth of burial and that very high rates of porosity reduction typically occur in the upper 1 km, probably owing to rapid losses of water in loosely compacted sediments (Rieke and Chilingarian, 1974; Chilingarian and Wolf, 1975, 1976; Füchtbauer, 1974; Schmidt and McDonald, 1979). On the basis of a compilation of porosity data from wells, Magara (1980) suggested that sandstones lose porosity linearly as a function of depth rather than exponentially. The well data that he cited are, however, from about 1 to 5 km below the surface. At these depths, the exponential porosity curves we assume for sandstones are so nearly linear (Fig. 2) that they easily can be fit to the sandstone porosities compiled by Magara (1980) within the scatter of data points. For the minimum limit (dashed curves in Fig. 2), we assumed that the surface porosity in each lithology except noncalcareous shale should be re-
duced along a single exponential curve, bu
surprisingly few data are available on the quanti-
tative relation between cementation and porosity
reduction with depth. An exponential decrease in
porosity with depth in limestones and dolomites
has been reported recently by Schmoker and
Halley (1982) for drilled Jurassic to Holocene
carbonate sequences in south Florida, where
cementation is active (Fig. 2). The curve for the
minimum limit in noncalcareous shales has two
exponential segments as required by our as-

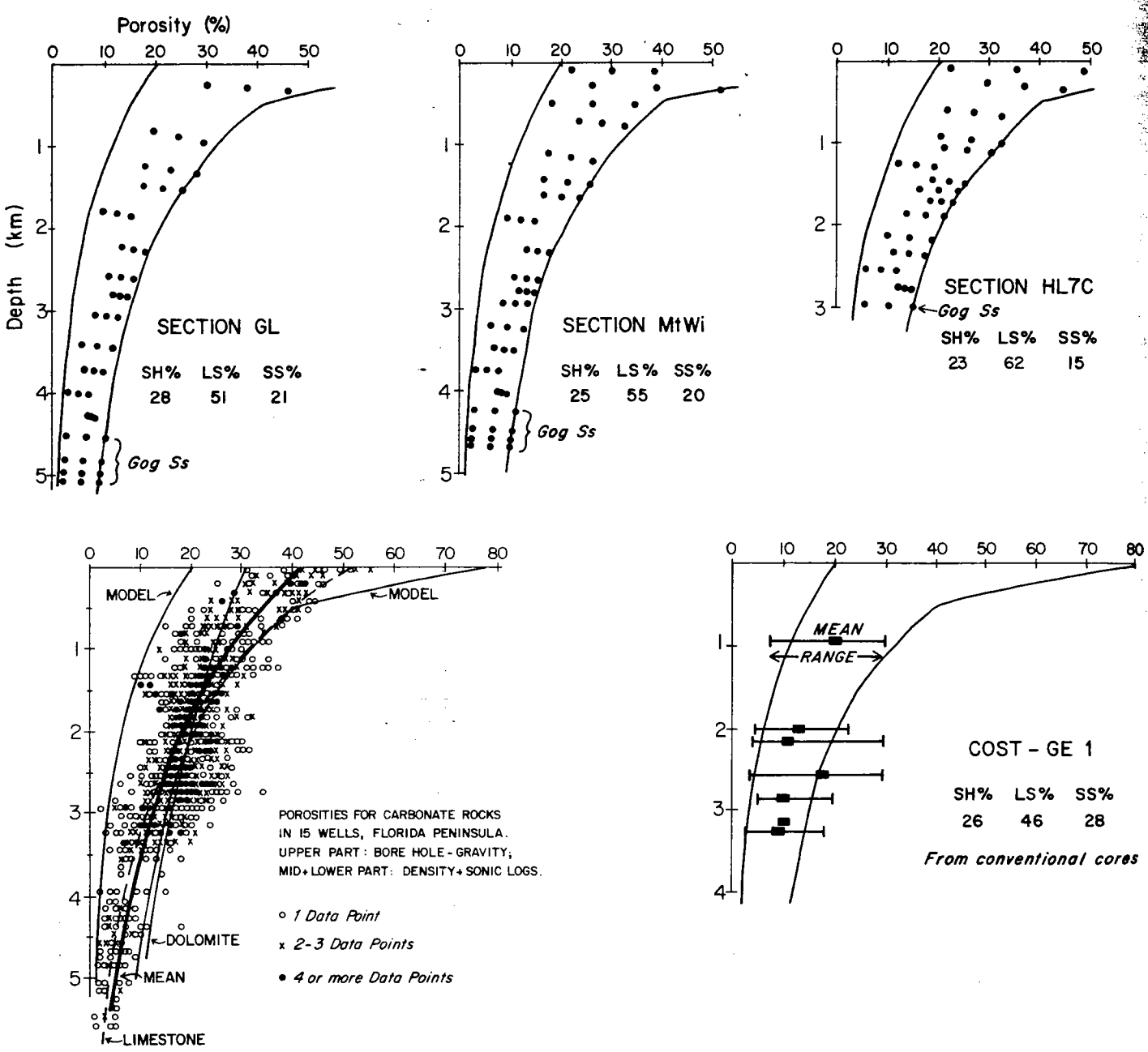

Figure 3. Test of the delithification procedure that is applied to miogeoclinal strata. Graphs in the top row show synthetic porosity-depth values calculated for three sections of Cambrian to Ordovician strata in the miogeocline using the delithification procedures described in the text. Location of the three sections is shown in Figure 4. Graphs in the bottom row compare porosity-depth values from wells in south Florida and offshore in the COST GE-1 well with ranges of synthetic porosities for the three miogeoclinal sections in the top row.

sumption that shales lacking carbonate impurities are not likely to be cemented and will lose porosity mainly by compaction (Von Engelhardt, 1973; Zankl, 1969; Rieke and Chilingarian, 1974). The exponential decay constants for the maximum and minimum curves were obtained from the upper and lower limits, respectively, for the range in measurements of porosity loss with depth for coarse- to fine-grained sediments in compilations of data from numerous drill holes in modern basins (Magara, 1980; Schmoker and Halley, 1982; Chilingarian and Wolf, 1975, 1976; Rieke and Chilingarian, 1974; Maxwell, 1964; Füchtbauer, 1974; Scholle, 1977; Von Engelhardt, 1973; Van Hinte, 1978).

Test of Delithification Procedures

To test the validity of our procedures for delithification, we calculated porosity versus depth profiles for three representative sections in the miogeocline. We compared the profiles with porosities measured in wells drilled in the southeastern Atlantic margin of the United States in the south Florida peninsula (Schmoker and Halley, 1982) and off the Florida coast (COST GE-1 well) (Halley, 1979), where the drilled sequences have essentially the same proportions of limestones, dolomites, shales, and clean sandstone as in the three miogeoclinal sections. Using our delithification procedures, we calculated three porosities for each formation in each section, one for the minimum delithification, one for the maximum delithification, and a third for the middle of the range between the two extremes. Each set of three porosities is plotted against the corresponding decompacted depth to the middle of each formation (Fig. 3). The plots show the predicted porosities as a function of depth at the time the most recent bed in the youngest formation was deposited. The scatter of points is an approximation of the range of porosities as a function of depth that would occur if the lithologies had been lithified by processes that spanned the extremes we have assumed for early cementation and for mechanical compaction.

The calculated porosities for the sections in the miogeocline correspond reasonably well to the downhole porosities for carbonate rocks in the modern carbonate margin (Fig. 3). The misfit with low porosities between about 1.5 and 3.5 km in the wells of south Florida (Fig. 3) occurs in lithologies composed mainly of dolomite (Schmoker and Halley, 1982). However, delithifying dolomites in the miogeoclinal sequences using the best-fit exponential for dolomite as determined by Schmoker and Halley (Fig. 3), instead of our exponentials for limestones, does not significantly change the values for delithification. We have not included estimates of the effects of secondary porosity formation, which can be anticipated at depths below about 1 km, and we have ignored the possibility of overpressuring. Even so, we consider the similarity between the calculated porosities in the carbonate bank and those in the modern margin as evidence that the maximum and minimum limits we have assumed for delithification are not unreasonable and that an acceptable approximation of the true changes in sediment thicknesses and densities during burial lies between the limits.

SUMMARY OF THE GEOLOGIC SETTING AND STRATIGRAPHY IN THE MIOGEOCLINE OF THE SOUTHERN CANADIAN ROCKY MOUNTAINS

The oldest sedimentary rocks in the miogeoclinal belt of the southern Canadian Rocky Mountains are in the Belt-Purcell Supergroup (Figs. 4, 5), which is Helikian in age (1,800 to 1,500 Ma) and has a maximum exposed thickness of about 15 km. This supergroup was interpreted by Gabrielse (1972), Stewart (1972), and Sears and Price (1978) as a continental terrace and aulacogen complex formed along an early proto-Pacific passive margin in western North America. Harrison and Reynolds (1976), however, suggested that it may have been deposited in epicontinental basins in the western United States. In Canada, the Belt-Purcell Supergroup was uplifted, deeply eroded, and locally metamorphosed during the East Kootenay–Racklan Orogeny, a poorly understood deformational event that is thought to have occurred between 1,300 Ma and 1,350 Ma (Leech, 1962; Young and others, 1979; McMechan and Price, 1982).

The Belt-Purcell Supergroup is overlain with angular unconformity by the Windermere Supergroup (Figs. 4, 5), which is Hadrynian in age (800 Ma to 575 Ma) and has a maximum thickness of about 9 km (Gabrielse, 1972). In the southern Canadian Rockies, this supergroup is regarded as a syntectonic complex that accumulated during an episode of high-angle faulting and differential subsidence that affected the central and western parts of the miogeocline between 800 and 900 Ma (McMechan and Price, 1982; Poulton and Simony, 1980; Monger and Price, 1979; Young and others, 1979; Brown and others, 1978). Mafic intrusive and extrusive rocks near the base of the Windermere Supergroup in the southern part of the Kootenay Arc (Fig. 4) are thought to have been extruded along deep crustal fractures that were active during this time (Monger and Price, 1979; McMechan and Price, 1982).

Above the Windermere Supergroup lies the extensive lower Paleozoic miogeoclinal wedge in which our analyses of subsidence were concentrated. The wedge is bounded at the top and base by regional unconformities (Fig. 5), between which the strata have a maximum exposed thickness of about 6 km and consist of distinct and laterally persistent facies. Resting on the sub-Cambrian unconformity is a thick deposit of Early Cambrian age composed for the most part of mature, shallow-marine quartz sandstones in the Gog, Cranbrook, and Hamill Groups (Fig. 5). Above these Early Cambrian sandstones, from near Cranbrook northwestward to at least 53° latitude, the inner part of the miogeocline consists of two major northwest-trending facies. The eastern facies is Middle Cambrian to Late Ordovician in age and constitutes a westwardly thickening prism of predominantly subtidal to supratidal carbonate deposits informally known as the carbonate bank (Aitken, 1966, 1971) (Figs. 4, 5). The western facies, Middle Cambrian to Middle Ordovician in age, occupies a trough informally known as the shale basin (Figs. 4, 5). This facies consists of shales, calcareous shales, and subordinate amounts of limestone and dolomite deposited in environments ranging from supratidal to middle or outer neritic (Aitken, 1978; McIlreath, 1974; Cook, 1970). The boundary separating the two facies is a narrow belt of algal complexes, the Kicking Horse Rim (Aitken, 1971). Farther west, in the Hughes Block, is a third facies, which is in thrust contact with the shale basin (Figs. 4, 5). Here, the lower Paleozoic sequence is a thin, predominantly shallow-water carbonate succession that was deposited on an uplifted block or arch of basement along the outer part of the miogeocline. West of the Purcell Anticlinorium, the lower Paleozoic strata consist of multiply deformed metasedimentary and metavolcanic rocks that lie principally within the Selkirk Allochthon in the Kootenay Arc and along the east flank of the Monashee Complex (Figs. 4, 5). The relation of the rocks in the Kootenay Arc to the miogeoclinal facies to the east is unclear. Although they have been regarded as a western facies of the miogeocline (Ross, 1970; Read, 1973, 1975; Okulitch, 1974, 1975), the strata of the Lardeau Group (Fig. 5) are now included in a suspect terrane (Coney and others, 1980).

SELECTION OF STRATIGRAPHIC DATA AND RADIOMETRIC TIME SCALE

The strata that are best suited for an analysis of tectonic subsidence are in the carbonate bank facies between the sub-Cambrian and sub-Devonian unconformities (Fig. 5). In this facies, the lithologies, ages, and correlations are well

established (Aitken, 1966, 1978; Aitken and Greggs, 1967) and penetrative cleavages are generally absent except near the major thrust faults (Cook, 1975; Price and Mountjoy, 1970). A minor development of stylolites occurs in some of the carbonate rocks, especially dolomites, but they are not common enough to suggest that solution has significantly reduced the original stratigraphic thicknesses. An additional advantage of using this facies is that the strata were deposited in middle- to inner-shelf environments, probably in water depths less than 100 m (Aitken, 1966, 1978), and water depth corrections (Wd in equation 1 and Fig. 1) are not required in calculating the tectonic subsidence. West of the carbonate bank in the shale basin and Hughes Block, the early Paleozoic strata are unsuitable for analysis owing to formation of widespread penetrative deformations and uncertain stratigraphic ages in parts of the sections. The late Precambrian strata below the

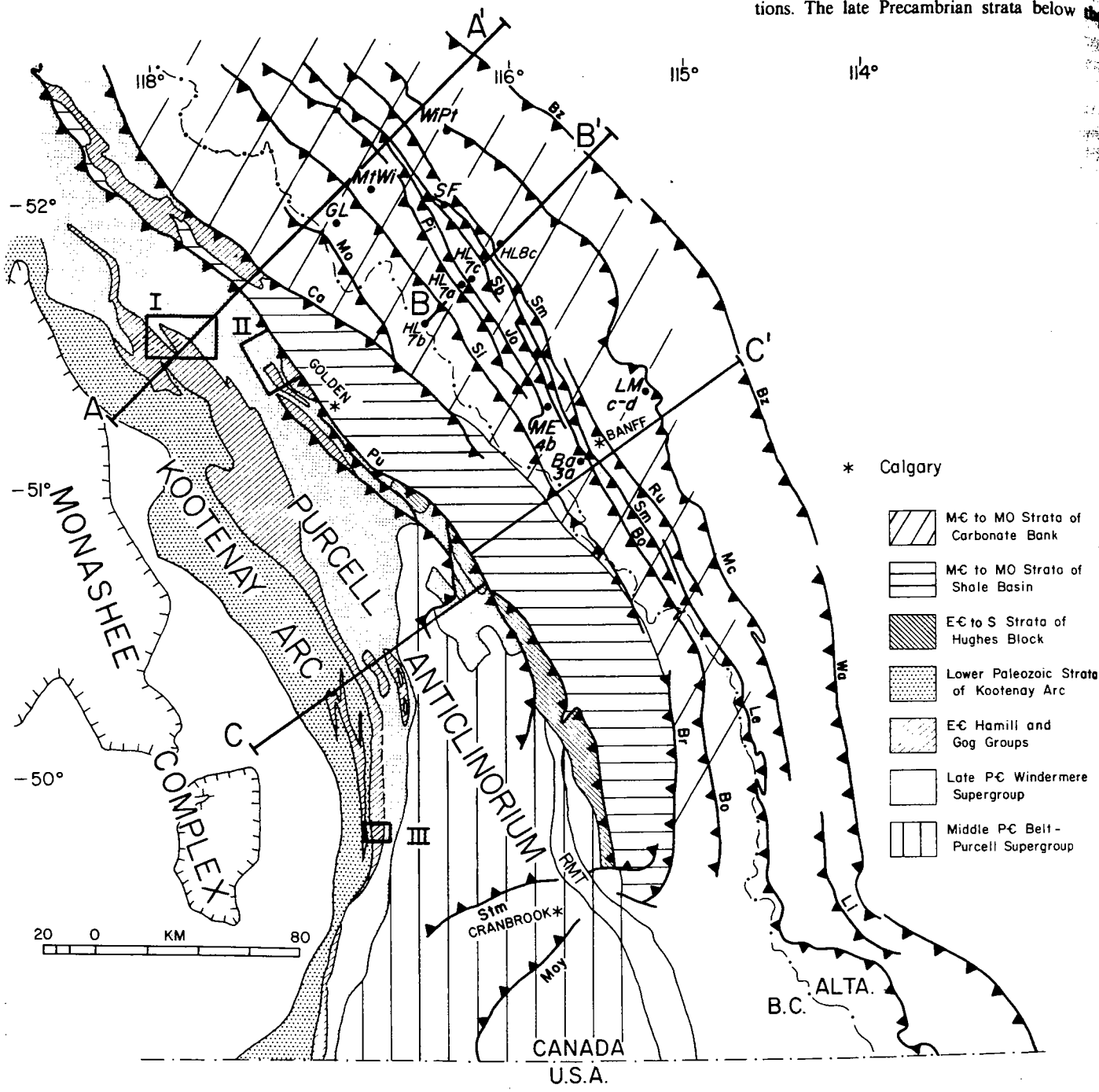

Figure 4. Map showing major late Mesozoic and early Tertiary structures and early Paleozoic depositional elements in the southern Canadian Rockies. Solid dots that are labeled with slanted abbreviations (WiPt, and so forth) are locations of columnar sections used to construct the tectonic subsidence curves. Thrusts are as follows: Bz, Brazeau; Mc, McConnell; Li, Livingstone; Ru, Rundle; Le, Lewis; Sm, Sulphur Mountain; Bo, Bourgeau; Sb, Sawback; Jo, Johnston Creek; Pi, Pipestone Pass; Si, Simpson Pass; Br, Bull River; Mo, Mons; Ca, Chatter Creek; Pu, Purcell; Stm, St. Mary; Moy, Moyie. AA′, BB′, and CC′ are locations of palinspastically restored sections of the carbonate bank shown in Figure 6. Locations of mafic rocks in the Hamill Group indicated by open rectangles labeled I, II, III. RMT, Rocky Mountain Trench. From Price (1980) and Price and Mountjoy (1970).

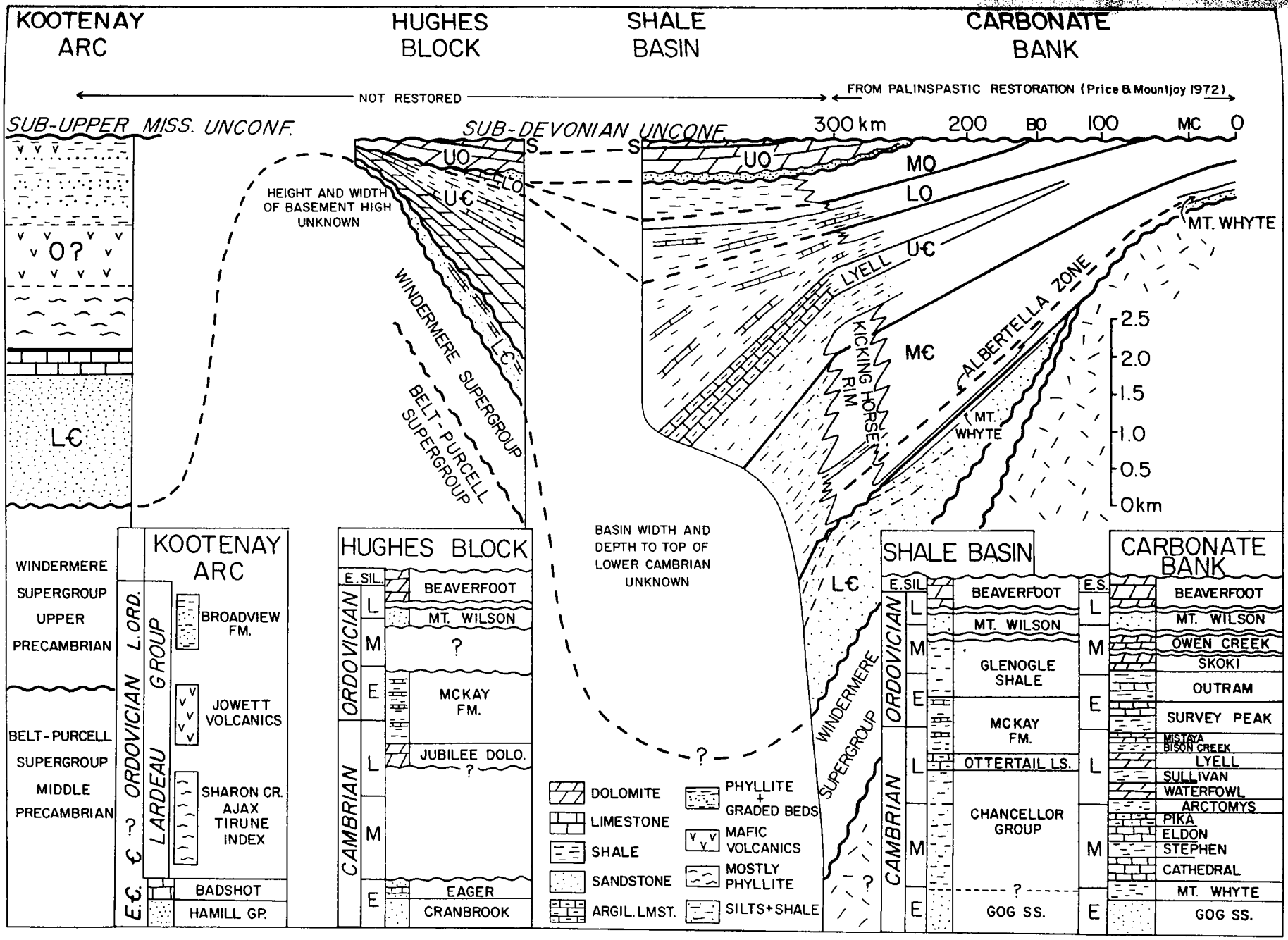

Figure 5. Diagrammatic cross section from the craton edge west of Calgary to the Kootenay Arc. Mc, McConnell Thrust; Bo, Bourgeau Thrust as located in restored section AA′ (Fig. 4); from Price and Mountjoy (1970). Data from Aitken (1971, 1978); Read (1973); Leech (1965); Fyles and Eastwood (1962).

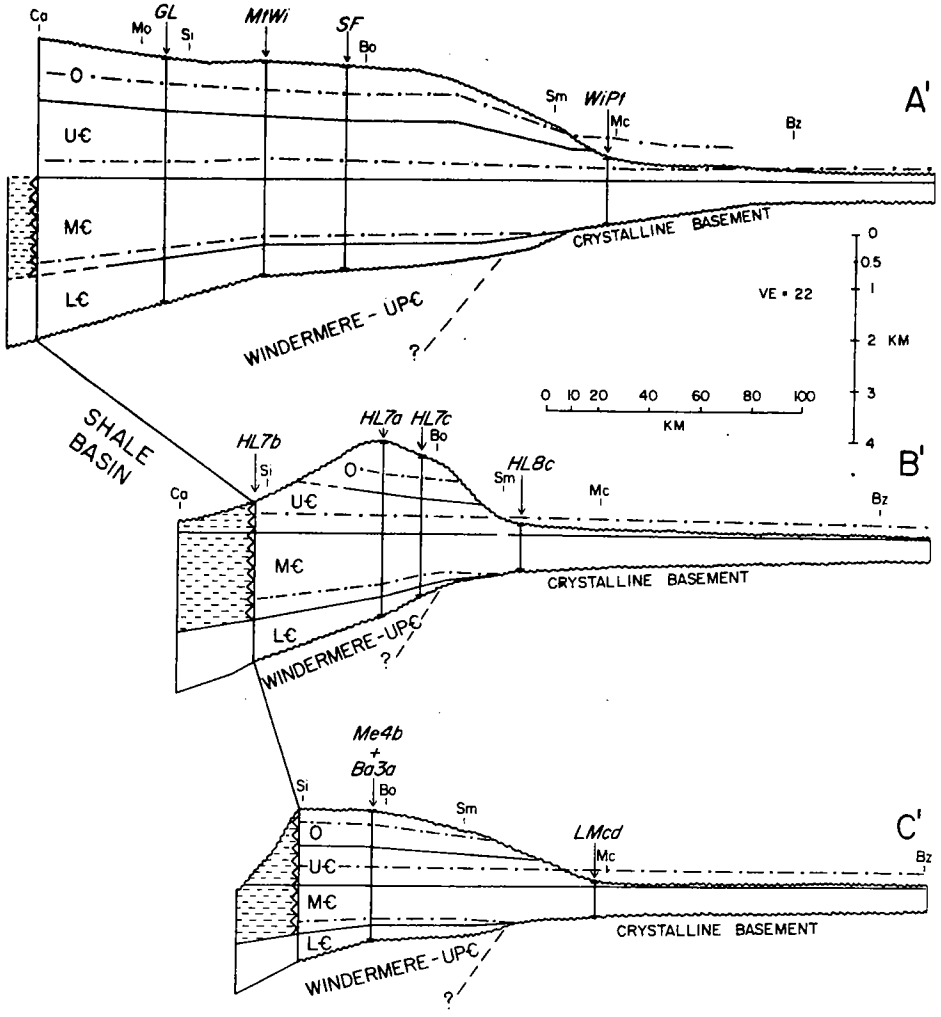

Figure 6. Palinspastic restorations of the carbonate bank facies, southern Canadian Rockies. Section lines A′, B′, and C′ are located in Figure 4. Arrows give approximate positions of columnar sections used for analysis (Fig. 4) after projection into the restored section. Bz, Mc, Sm, and so forth are restored positions of intersections of thrusts in the upper plate and the ground surface. Dash-dot lines are delithified thicknesses of (from bottom to top) Lower Cambrian, Lower to Middle Cambrian, and Lower to Upper Cambrian intervals. Section A′ is from Price and Mountjoy (1970); B′ constructed from map cross sections in Price and Ollerenshaw (1971a, 1971b) and Ollerenshaw (1967); C′ from Price (1980).

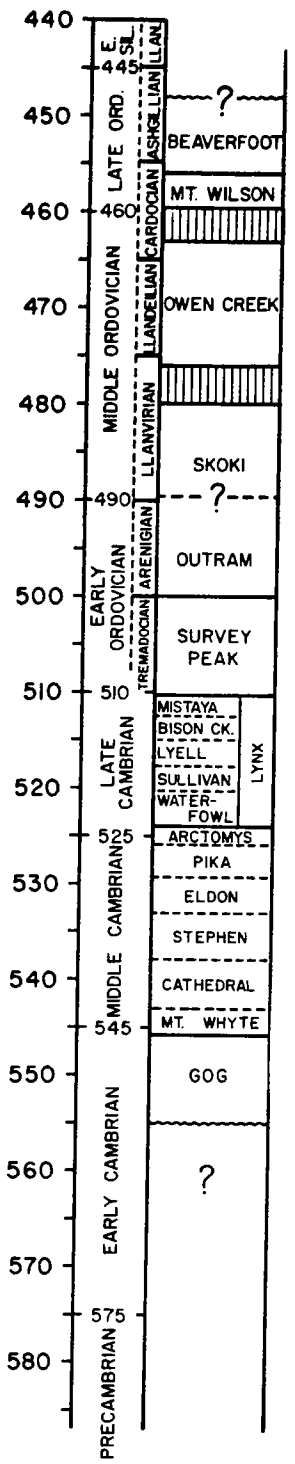

Figure 7. Stratigraphic columns giving faunal and radiometric ages of lithologic units used for construction of tectonic subsidence curves. Vertical lines indicate unconformities. The specific radiometric ages for stratigraphic boundaries that were used to construct the curves appear within the left-hand column between the series names (Early Cambrian, Middle Cambrian, and so forth).

basal quartz sandstones in the carbonate bank also are unsuitable because of uncertain correlations and lack of radiometric dates.

Stratigraphic columns that lie between major thrust faults (Figs. 4, 6) were selected for analysis in order to avoid errors due to thickness changes and uncertain correlations across these faults. An additional criterion in choice of columns was their proximity to palinspastically restored cross sections of the carbonate bank (Figs. 4, 6). This allowed the distances between the columns prior to deformation to be estimated by projecting them along strike into the nearest restored section (Fig. 6). Stratigraphic thicknesses and percentages of lithologies in the formations (Table 1) are from our field studies and from published structural cross sections and published measured sections in Aitken and Greggs (1967), Aitken and Norford (1967), Norford (1969), Aitken (1966), Price and Mountjoy (1971, 1972a, 1972b, 1972c, 1972d, 1978a, 1978b, 1978c, 1978d). The stratigraphic ages (Fig. 7) for the sections are from Aitken and Greggs (1967), Aitken and Norford (1967), Norford (1969), Aitken (1968), and Aitken and others (1972).

The correct time scale for the early Paleozoic is uncertain (see Harland and Francis, 1971, and

TABLE 1. THICKNESS AND SECTION

Formation	GL	MtWi	SF	WiPi	HL7b	HL7a	HL7c	HL8c	Ba3a	ME4B	LMc-d
Gog	810	580	448	..	1041	296	258	..	303	353	..
Mt Whyte	89	137	124	..	109	124	114	69	101	121	90
Cathedral	453	366	376	152	555	247	312	248	247	262	169
Stephen	81	122	89	64	99	74	50	30	50	76	45
Eldon	465	381	322	238	570	336	297	228	267	262	209
Pika	222	151	183	97	272	242	188	89	101	156	95
Arctomys	235	112	124	64	223	109	99	84	86	101	50
Waterfowl (L. Lynx)	166	184	149	28	..	109	123	50	96	151	[70
Sullivan (L. Lynx)	424	376	99	82	..	74	50	89	45	65	
Lyell (U. Lynx)	344	304	[505	[85	..	306	297	[178	288	353	
Bison Creek (U. Lynx)	202	192			..	50	25		101	111	..
Mistaya (U. Lynx)	161	102			..	153	173		91	126	..
Survey Peak	488	396	381	..	..	381	347	..	373	338	..
Outram	443	258	158	..	..	183	173	..	151	116	..
Skoki	..	140	173	..	..	173	148	..	..	..	..
Owen Creek	..	187	99	..	..	124	..	..	..	..	..
Mt Wilson	..	171	..	..	..	74	..	..	..	..	..
Beaverfoot	..	..	..	..	..	..	..	..	..	..	..

Outcrops in bank

Note: thickness is in metres. See Figure 4 for locations.

Fitch and others, 1976, for review). The radiometric ages for the stratigraphic boundaries in the sections (Fig. 7) are from the time scale of Armstrong (1978), which is based on a large and well-documented set of radiometric data. Other time scales, which differ from that of Armstrong, were proposed recently by Cowie and Cribb (1978), McKerrow and others (1980), Gale and others (1979, 1980), and Harland and others (1982). However, we used each of these time scales to construct tectonic subsidence curves for the miogeocline and found that the differences in durations of the dated intervals are not great enough to significantly change the shapes of the curves obtained using the Armstrong scale. On the basis of discussions of interprovincial faunal correlations for the early Paleozoic in Sweet and Bergstrom (1976), Williams (1976), Robinson and others (1977), Landing and others (1978), and Cowie and others (1971), we assumed a ±5-m.y. uncertainty in the correlation of strata in the southern Canadian Rockies with the biostratigraphic units, chiefly in Britain, to which the radiometric ages on the Armstrong time scale are assigned. We estimated the length of time represented by the unconformities in the Ordovician (Figs. 7, 8) by comparing the radiometric ages with sedimentary thicknesses and the approximate sizes of the faunal gaps reported by Norford (1969) and Aitken and Norford (1967).

COMPARISON OF TECTONIC SUBSIDENCE IN THE CARBONATE BANK FACIES WITH THE POST-RIFT SUBSIDENCE IN PASSIVE MARGINS

Subsidence in Modern Passive Margins

In terms of the passive margin model for the Cordilleran miogeocline, the carbonate bank, with its widespread shallow-marine facies, wedge shape, and tectonically stable depositional environments, is regarded as part of the sedimentary prism deposited during the drift or post-rift stage of the proto-Pacific margin (Stewart, 1972; Burchfiel and Davis, 1975; Monger and Price, 1979). The tectonic subsidence in the carbonate bank, therefore, should be comparable with post-rift tectonic subsidence in modern passive margins.

Subsidence curves have been constructed for the sedimentary wedges in the modern Atlantic margins of northeast Canada (Keen, 1979); the northeastern United States (Watts and Ryan, 1976; Watts and Steckler, 1979); western Spain, France, and Britain (de Charpal and others, 1978); and northwest Africa (Hardenbol and others, 1981). The post-rift subsidence curves in these margins have been found to closely resemble the age-depth curves for oceanic crust. This result is considered to be strong evidence that thermal cooling of the lithosphere is the primary cause of subsidence in passive margins following the onset of sea-floor spreading (Watts, 1981; Keen, 1982).

Different models have been proposed recently to explain both the observed subsidence and thermal histories of modern passive margins on the basis of differing assumptions regarding the behavior of the lithosphere during the rifting stage (McKenzie, 1978; Royden and Keen, 1980; Beaumont and others, 1982; Jarvis and McKenzie, 1980; Cochran, 1981; Royden and others, 1980). There are relatively large differences in the heat flow and subsidence calculated from these models in the first 10 to 20 m.y. after onset of drift because of the different initial temperature conditions required by each model for the time at which rifting ends. After the first 10 to 20 m.y., however, the subsidence curves for the models are similar and have the same form as the age-depth curves for ocean floor. This form consists of a segment that is linear with respect to the $\sqrt{\text{time}}$ for several tens of millions of years followed by a segment that decays exponentially approaching an asymptotic value (for example, see Fig. 9). Consequently, beginning about 10 to 20 m.y. after rifting, subsidence curves calculated from any of the thermal-mechanical models of passive margins should be suitable for comparison with the tectonic subsidence curves from the carbonate bank.

Comparison with Post-Rift Subsidence Calculated from the McKenzie Stretching Model

The simplest model for passive margins is the one-dimensional stretching model of McKenzie (1978). This model is based on the assumption that the lithosphere is stretched uniformly and instantaneously by horizontal extension during rifting. The stretching thins the lithosphere, causing passive upwelling of the asthenosphere and passive heating by reduction of the distance between isotherms. At the onset of drift, the lithosphere cools, contracts, and subsides at a rate that is proportional to the amount of extension (β) or thinning ($1/\beta$) that has occurred. In the limit, if the lithosphere were thinned to zero thickness, the subsidence and heat flow would be identical to those of oceanic crust.

In Figure 8, the tectonic subsidence we have calculated for the sections in the carbonate bank is compared with the post-rift tectonic subsidence curves calculated from the stretching model of McKenzie for different amounts of stretching (β). The stretching model was calibrated for 5 km of oceanic crust following Steckler (1981) and Cochran (1981) and the asymptotic values for the final depths of the curves were calculated for an equilibrium thermal thickness of 125 km for the lithosphere (Parsons and Sclater, 1977). Other parameters used in the model are from McKenzie (1978). The amount of subsidence that would occur during extension (the initial subsidence in the McKenzie model) is not included in the model curves in Figure 8, and so the initial depth of the curves is zero at the time at which extension ends and thermal contraction begins. In each model curve, the segment that is a linear function of the $\sqrt{\text{time}}$ extends from about 16 to 70 m.y. after subsidence begins, and the exponential segment, which begins at 70 m.y., has a decay constant of 62.8 m.y. The tectonic subsidence curves calculated from the sections in the carbonate bank facies are fit by eye to the subsidence curves constructed from the extension model (Fig. 8). The fit is made

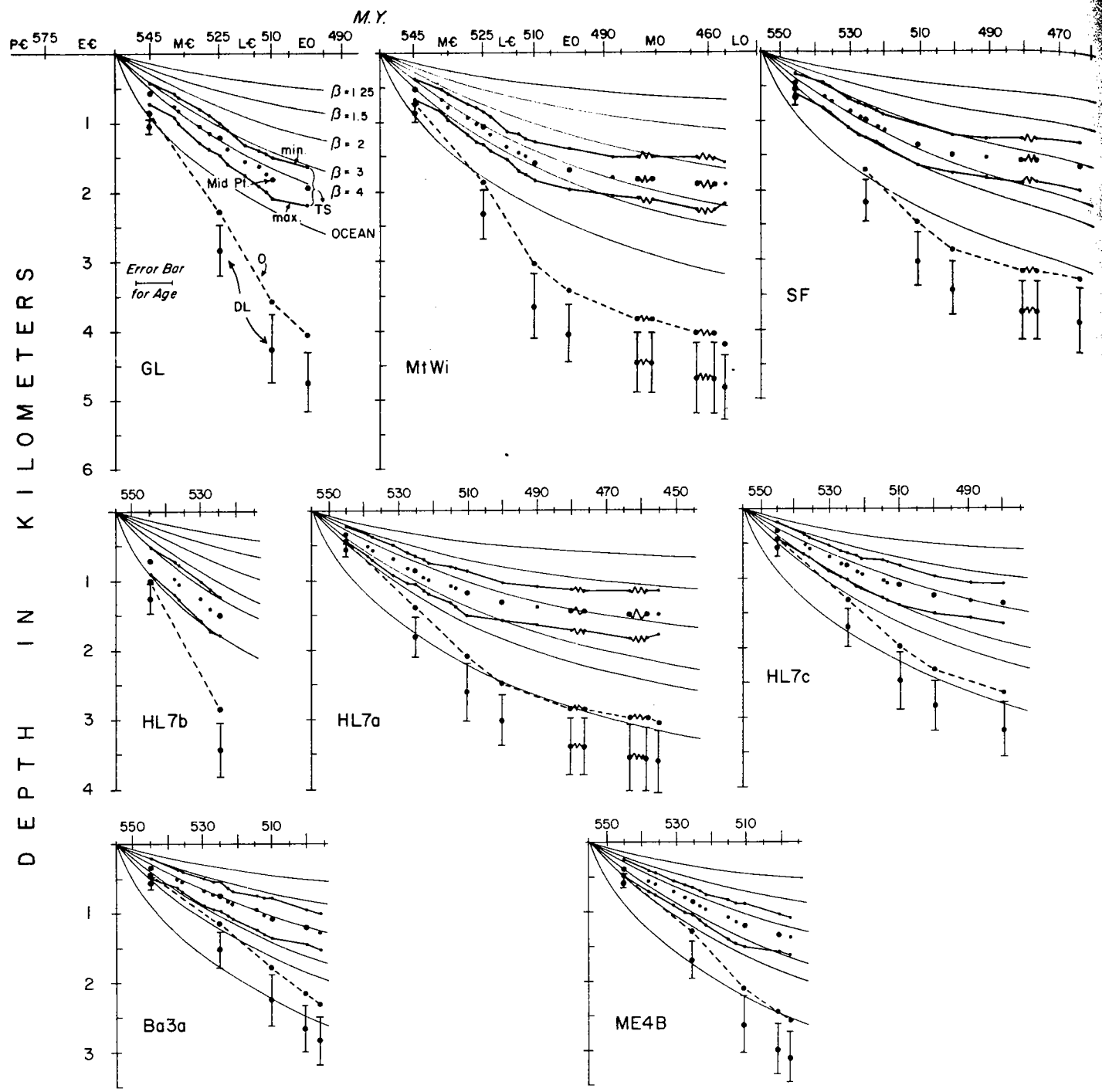

Figure 8. Results of analyses of subsidence in the stratigraphic columns from the carbonate bank facies. Locations of columns are given in Figure 4, and their relative positions in restored cross sections are given in Figure 6. Solid lines are post-rift subsidence curves calculated from the McKenzie (1978) stretching model. Dashed line (0) is cumulative thickness curve for observed or present-day stratigraphic thicknesses. For the cumulative thickness curves, the vertical axis should be read as stratigraphic thickness in kilometres. Vertical bars (DL) are ranges between maximum and minimum delithified thicknesses. The ranges are shown only for stratigraphic boundaries that have radiometric ages assigned to them by Armstrong (1978). Heavy solid lines are tectonic subsidence curves (TS) for the maximum (lower) and minimum (upper) limits of delithification. Points that the solid lines connect correspond to tops of formations given in Table 1. Dots give the tectonic subsidence for the mid-points between the two limits. Large dots are the formation boundaries to which radiometric ages are assigned on the Armstrong time scale. Small dots are formation boundaries that do not have radiometric ages and are positioned by interpolation between the large dots. Note the good fit between the curves calculated from the model for post-rift thermal contraction and the upper, lower, and middle points of the tectonic subsidence for the carbonate bank. The β values to which the tectonic subsidence data correspond should not, however, be interpreted as a measure of the amount of crustal thinning.

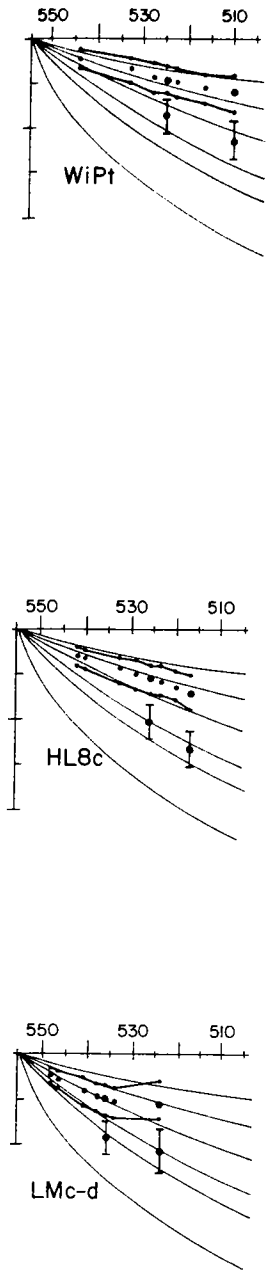

Figure 8. (*Continued*).

using the mid-points of the ranges for delithification and ages. In that the age of the base of the Gog Group (that is, the base of the sections) is not known, the points are fit to the curves beginning at the base of the Middle Cambrian, which is the oldest stratigraphic boundary with a radiometric age (545 Ma).

It is clear in Figure 8 that a good fit can be found between the form of the curves from the model of post-rift thermal contraction and the form of the tectonic subsidence curves from the carbonate bank at the mid-points between the limits of delithification. It is also evident that the curves given by the maximum and minimum limits fit the model curves. In all cases, the best fit appears to occur in the segments of the model curves that are linear with respect to the $\sqrt{\text{time}}$, or between about 545 Ma and 485 Ma.

Although the ranges between the limits for the tectonic subsidence curves are not small, those ranges cannot be treated strictly as error bars. If delithification factors were specified for each of the units in a section, the form of the tectonic subsidence curve for that section could fluctuate by about 40%, at most, of the distance between the limits, and this amount of variation cannot occur between any two successive units but only over the full length of the curve. The maximum variation in the curve that can occur between any two successive points is about 15% of the distance between the limits. This is the case because once the delithification factors are specified for a certain unit in a section, lithification of the strata in that unit no longer contributes to the calculation of the range between maximum and minimum limits at the time of deposition of the higher units in the section. In other words, the tectonic subsidence curve for a section can lie along the minimum limit, along the maximum limit, or somewhere between the two limits and nearly parallel to them. Regardless, then, of which delithification factors are applied to the units in the sections in the carbonate bank, the form of the tectonic subsidence curves will correspond closely to the form of the post-rift subsidence curves calculated from the McKenzie model.

Before the results in Figure 8 can be interpreted in terms of subsidence mechanisms, the effects of two simplifying assumptions involved in constructing and comparing the model curves and the tectonic subsidence curves must be considered. First, the model curves were calculated from a one-dimensional passive-margin model, but two-dimensional processes, such as flexure and lateral heat flow, are known to have an important effect on the subsidence in modern margins (Steckler and Watts, 1982; Karner and Watts, 1982; Beaumont and others, 1982). Steckler and Watts (1982) and Beaumont and others (1982) have shown, however, that the form of the subsidence curves calculated from a one-dimensional extension model is not changed by adding the effects of flexure and lateral heat flow; that is, the post-rift subsidence curves for two-dimensional models with flexure and lateral heat flow included have an initial complex form followed by a segment that is linear with respect to the $\sqrt{\text{time}}$ and an exponential segment that approaches an asymptotic value (see Fig. 9). Addition of flexure and lateral heat flow, however, does change the slope of the $\sqrt{\text{time}}$ segment and the asymptotic depth that the curves approach relative to the one-dimensional models. This means that the β values corresponding to the tectonic subsidence curves in Figure 8 cannot be used to calculate the amount of extension or heating during rifting.

Second, the effects of lateral heat flow and flexure, which must have been active during subsidence in the miogeocline, were ignored in calculating tectonic subsidence from equation 1. The basement response function (Φ) in equation 1 was set equal to one, and the subsidence caused by the weight of sediment in each unit was removed using a simple Airy type of isostatic model. This is equivalent to assuming that the lithosphere has no lateral strength with respect to the size of the sedimentary load in the miogeocline. It can be inferred from two-dimensional extension models of passive margins, however, that this simplification should not be a serious difficulty as long as only the form of the subsidence curves is of interest (Steckler and Watts, 1982; Steckler, 1981). To demonstrate this point, we used a two-dimensional extension model (Steckler, 1981; Steckler and Watts, 1982) to construct two hypothetical passive margins in which flexure and lateral heat flow are active (Fig. 9). One of these is a simple margin constructed by assuming uniform stretching of the lithosphere, proposed by McKenzie (1978). The other is a complex margin with an unconformity and an outer ridge that were constructed using the depth-dependent extensional (or thinning) mechanism proposed by Royden and Keen (1980). The depth-dependent mechanism was developed to explain the anomalously thin syn-rift deposits and formation of unconformities at the time of breakup in some margins. It differs from the McKenzie model in that the upper part of the lithosphere (taken to be crust in the model in Fig. 9) is stretched by a factor of δ, and the remainder is stretched by a factor β that is larger than δ by a specified amount (see Royden and Keen, 1980; and Beaumont and others, 1982, for discussion of this model and its application to margins). The fine-line curves in Figure 9 show the post-rift tectonic subsidence calculated from each model as a function of time. Using the two-dimensional model of Steckler (1981), both margins were progressively infilled with compacting sedimentary layers, so that the sediment-water interface remained at sea level. In both models, the flexural rigidity was estimated from the depth to the 450 °C isotherm, so that the rigidity of the margins would increase through time as the margin cooled and sediments were added (Watts, 1981; Steckler and Watts, 1982). Tectonic subsidence curves then were calculated for both of the sediment-filled margins, using an Airy type of isostatic model to remove the sediment loads

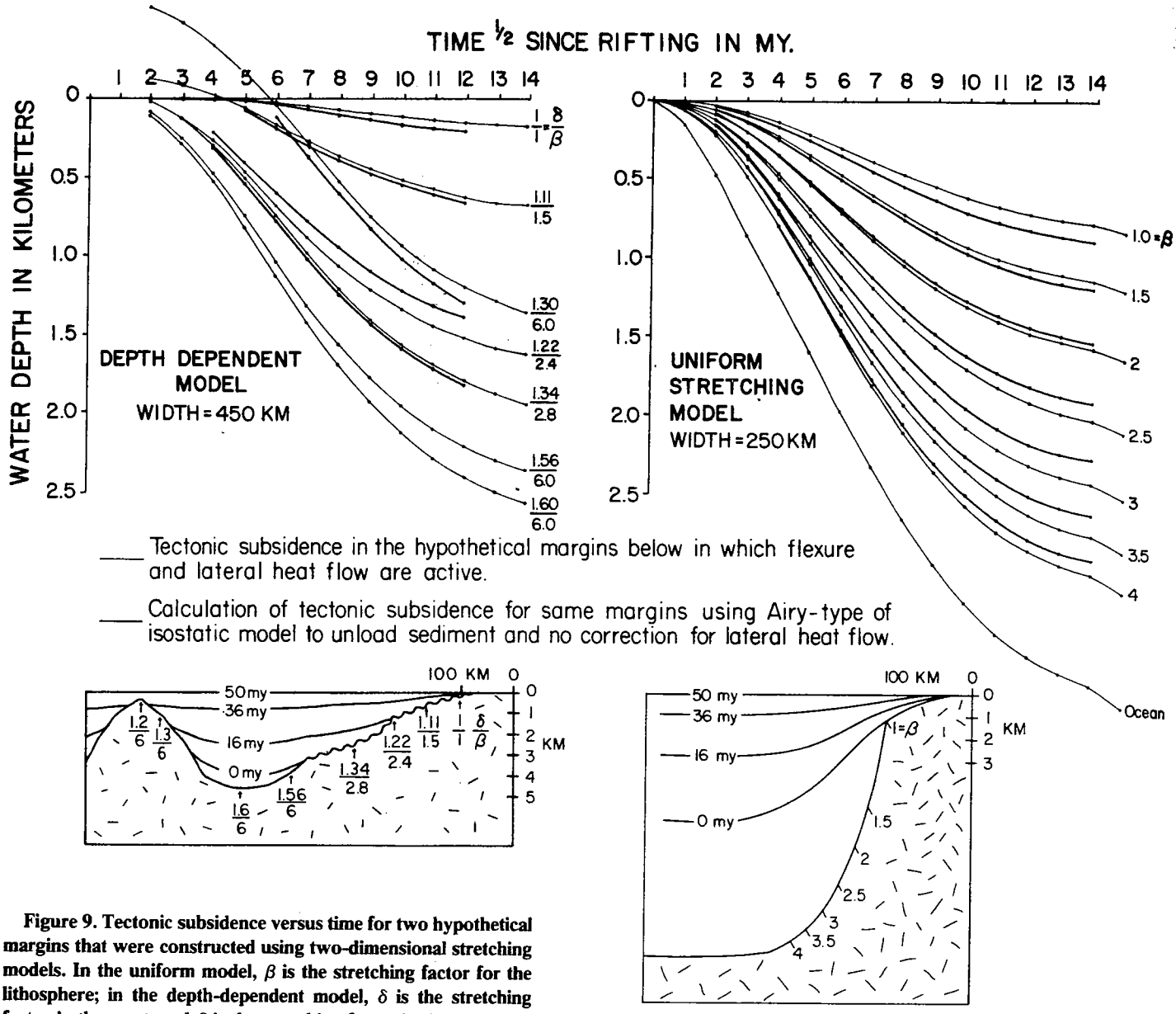

Figure 9. Tectonic subsidence versus time for two hypothetical margins that were constructed using two-dimensional stretching models. In the uniform model, β is the stretching factor for the lithosphere; in the depth-dependent model, δ is the stretching factor in the crust, and β is the stretching factor in the subcrustal lithosphere. Model parameters as in Steckler and Watts (1982). Light curves show tectonic subsidence calculated with flexure and lateral heat flow taken into account. Heavy curves show tectonic subsidence calculated using an Airy type of sediment-unloading model, with no correction for lateral heat flow. The two margins are shown with the sediment thickness that is produced by the model after 50 m.y. of post-rift thermal subsidence. The similarity between the two sets of curves for each model implies that using an Airy type of sediment-unloading model in a basin where flexure and lateral heat flow were active during subsidence does not introduce a serious error in recovering the form of tectonic subsidence.

and making no correction for lateral heat flow. The two sets of curves (flexural and Airy) have nearly the same form (Fig. 9). The difference, moreover, in depth between the Airy and flexural subsidence curves is smaller than the ranges between the limits that we assume for delithification. It would appear that for margins that have at least moderate widths (greater than about 100 km) and are filled with shallow-marine sediments, the largest errors in calculating the form and magnitude of tectonic subsidence are from uncertainties in delithification of the sedimentary units.

We conclude that the close similarity between the form of tectonic subsidence in the carbonate bank and the form of post-rift subsidence calculated from the simple extension model is not likely to be a coincidence resulting from the assumptions and simplifications involved in constructing the curves. The good fit with the segments of the model curves that are a linear function of the $\sqrt{\text{time}}$ is especially significant because that form of the post-rift subsidence depends only on cooling by diffusion of heat from the lithosphere and is independent of assumptions about rifting mechanisms and the equilibrium thermal thickness of the lithosphere (McKenzie, 1978). The similarity between the subsidence curves from the carbonate bank and the stretching model, therefore, is persuasive evidence that tectonic subsidence in the carbonate bank was controlled mainly by thermal contraction of heated lithosphere.

EVIDENCE FROM SUBSIDENCE CURVES FOR THE AGE OF BREAKUP AND FORMATION OF THE EARLY PALEOZOIC PROTO-PACIFIC MARGIN IN THE SOUTHERN CANADIAN ROCKIES

The thermal form of the subsidence curves from the carbonate bank places fairly narrow limits on the age for the end of rifting and the beginning of thermal contraction of the heated lithosphere. This age is significant because the end of rifting and the beginning of thermal contraction in a passive margin coincide with the age of breakup and onset of sea-floor spreading (Keen, 1979; de Charpal and others, 1978). The relatively high slopes in the early parts of the subsidence curves from the carbonate bank indicate relatively high rates of heat loss, implying that post-rift thermal contraction could not have been in progress for very long prior to about 545 Ma or Middle Cambrian time (Fig. 6). One method of estimating when thermal contraction began is simply to trace each tectonic subsidence curve back to zero water depth along the corresponding thermal subsidence curve that was calculated from the model. This yields a remarkably consistent age for the beginning of thermal contraction of 555 Ma, or mid-Early Cambrian, in all sections (Fig. 8), even though the sections have different thicknesses and are from both the inner and outer parts of the carbonate bank (Figs. 4, 6). The tectonic subsidence curves cannot be shifted horizontally to the right and fit to any of the model thermal curves, which suggests that 555 Ma is a probable minimum age for the beginning of thermal contraction. Essentially the same minimum age is indicated by the presence of widespread, tectonically stable marine deposits of late Early Cambrian and younger age in the miogeocline (Fig. 5) (Aitken, 1966, 1978). Each tectonic subsidence curve can be shifted down and to the right, however, and fit to a model curve with a higher β value, although the match is not as good as the preferred one shown in Figure 6. Fitting the curves to higher β values yields older ages for the beginning of thermal contraction and places some of the strata beneath the Gog Group within the post-rift phase of the margin. As rates of subsidence or heat loss in a passive margin cannot exceed the rate of subsidence or cooling of ocean floor, an upper limit for the time when thermal contraction began is given by fitting the subsidence curves to the thermal curve for oceanic crust. This yields an upper limit for the initiation of thermal contraction of about 600 Ma. On the basis of the form of the subsidence curves from the carbonate bank, therefore, breakup and onset of spreading in the proto-Pacific Ocean that was adjacent to the early Paleozoic margin in the southern Canadian Rockies occurred at some time between 555 Ma and 600 Ma or between latest Precambrian and earliest Cambrian time. It is interesting to note that a comparable age (about 675 Ma) for beginning of thermal contraction in the miogeocline in Nevada and southern California was suggested by Stewart and Suczek (1977) after fitting an exponential curve to the cumulative thickness curve for the strata of late Precambrian to Ordovician age.

The age for breakup inferred from the form of the subsidence curves is supported by limited but significant petrologic and stratigraphic data in the Hamill Group, a succession of latest Precambrian to Early Cambrian strata from 1 km to 3 km thick in the southern Canadian Rockies (Figs. 4, 5) (Simony and Wind, 1970) that has received relatively little attention in the published literature. In the northern Selkirk Mountains (locality I in Fig. 4), parts of the Hamill Group consist of pillowed mafic lavas, tuffs, and breccias as much as a few hundred metres thick interlayered with alternating shales and coarse-grained arkosic sandstones, some of which are graded and presumably were deposited in relatively deep water (Wheeler, 1963; Höy, 1979). In the Dogtooth Ranges (locality II in Fig. 4), the lower few hundred metres of the Hamill Group contains coarse-grained arkosic sandstones and conglomerates (Ellison, 1967), and the upper part contains pillowed mafic lava and breccia about 30 m thick (Simony and Wind, 1970). In the Purcell Anticlinorium between localities I and III (Fig. 4), the Hamill Group has been studied only in reconnaissance, but it appears to contain a vertical change from feldspathic conglomerates at the base to quartzose sandstones at the top (Reesor, 1973). In the Riondell area northwest of Cranbrook (locality III in Fig. 4), the Hamill Group consists of coarse-grained feldspathic sandstones overlain by quartz sandstones, phyllites, and schists, with a layer of amphibolite about 200 m thick in the lower or middle part of the section (Höy, 1977). Within a relatively large area of the miogeocline, then, strata correlative with the age we infer for breakup consist of coarse-grained arkosic sediments and scattered mafic lavas, an association that is suggestive of a continental terrane undergoing rifting.

In discussing the problem of late Precambrian rifting in the southern Canadian Cordillera, Monger and Price (1979) noted that all known high-angle faults are transverse, not parallel, to the trend of the miogeocline. These faults are inferred from large vertical stratigraphic separations in upper Precambrian strata in the east-trending St. Mary fault zone at the south end of the shale basin (Fig. 4) (Lis and Price, 1976; Benvenuto and Price, 1979). Transverse structures are not uncommon in modern rift zones and margins, however (Dewey and Burke, 1974; Burke, 1976). A speculative explanation for the development of the east-trending structures in the St. Mary fault zone is suggested by the presence of a large east-trending aulacogen, the Southern Alberta Aulacogen, which lies in the craton to the east on strike with the St. Mary fault zone (Fig. 10) (Kanasewich and others, 1969). Distinctive gravity and magnetic anomalies that are associated with the aulacogen have been traced southeastward beneath the thrust and fold belt into the St. Mary fault zone (Kanasewich and others, 1969). If the Southern Alberta Aulacogen is viewed as the failed arm of a triple junction, the east-trending high-angle faults along the St. Mary fault zone could be analogous to deep transverse fractures such as those within the Afar triple junction that lie on strike with the East African Rift System (Fig. 10). Although the Southern Alberta Aulacogen probably was formed in middle Precambrian time (Stewart, 1972, 1976; Sears and Price, 1978), late Precambrian and Early Cambrian(?) movement along the St. Mary fault zone could have been a result of reactivation of the east-trending structures at the time of rifting that initiated the early Paleozoic margin.

An age of 555 to 600 Ma for breakup and initiation of drift along the early Paleozoic passive margin raises an important question about the origin of an older episode of block faulting and mafic volcanism that initiated deposition of the Windermere Supergroup and has been regarded as part of a widespread rifting event (Stewart, 1972, 1976; Burchfiel and Davis, 1975; Dickinson, 1977). The age of this episode is thought to be 827 to 918 Ma, on the basis of limited K-Ar dating of mafic lavas near the base of the Windermere Supergroup in northeastern Washington (Miller and others, 1973). If this age is correct, a rifting event appears to have occurred more than 200 m.y. before the time we infer for rifting and breakup in the southern Canadian Rockies.

We can suggest two hypotheses that could account for the apparently long span of time between the older rifting event and the breakup inferred from the subsidence curves. First, the older rifting could have been part of an episodic process that spanned a considerable length of time before continental separation was accomplished, as, for example, in the Atlantic margins of northwestern Europe (Burke, 1976; Birkelund and others, 1974) and along the Indian Ocean margin of western Australia (Veevers and Cotterill, 1978). The extrusion of mafic volcanics at the base of the Windermere Supergroup could represent only an early phase of the

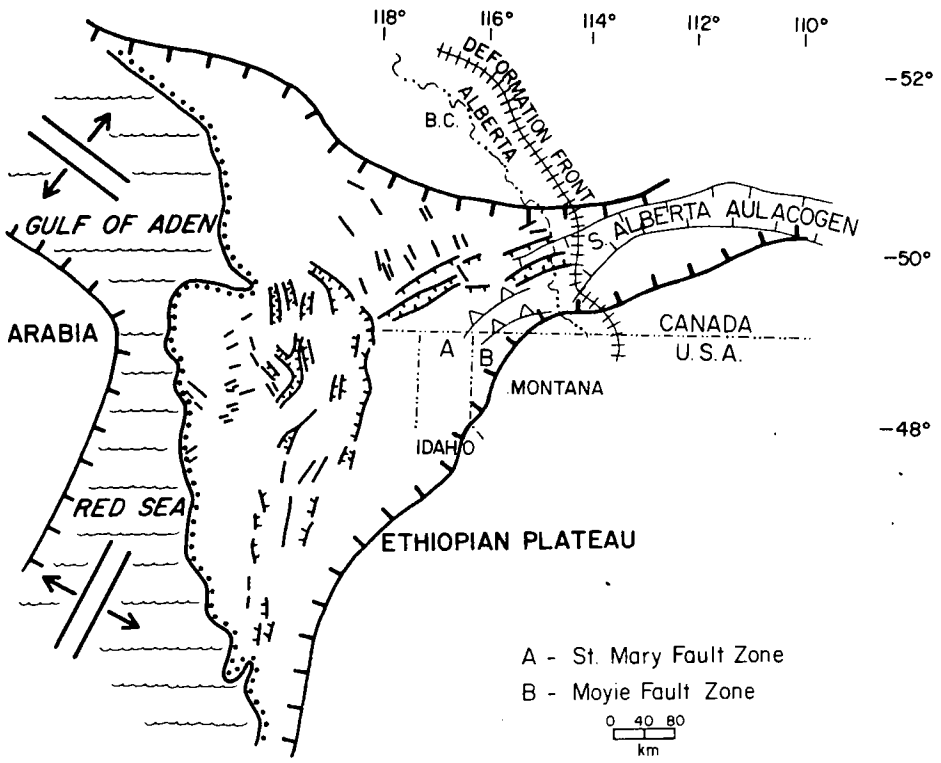

Figure 10. Comparison of the Afar region, East Africa, shown by heavy lines, with the Southern Alberta Aulacogen, the Late Cretaceous to early Tertiary deformation front, and the east-trending faults at the south end of the shale basin, all shown by light lines. Scale is the same for both regions. The Afar region has been positioned such that the East African Rift coincides with the Southern Alberta Aulacogen. Data for the Afar region are from Christiansen and others, 1975. Note that east-trending structures (A, B) in the northerly trending miogeocline are analogous to a major set of fractures in the triple junction that are parallel to the East African Rift. A passive margin formed by continued opening of the Gulf of Aden and the Red Sea would trend at a high angle to these fractures.

prolonged rifting. In this view, continental separation and formation of a proto-Pacific margin did not occur until a last phase of rifting was completed shortly before or during earliest Cambrian time.

A second hypothesis is that a complete sequence of rifting, continental separation, and growth of a proto-Pacific margin occurred entirely within the late Precambrian. In this view, the early Paleozoic miogeocline is a second continental margin wedge deposited after a second major rifting event in latest Precambrian or earliest Cambrian time that only modified the existing proto-Pacific margin. If this is correct, the Windermere Supergroup should consist of an extensive syn-rift complex passing upward into a widespread post-rift deposit (except where removed by erosion along the sub-Cambrian unconformity), and a second syn-rift complex should lie between the Windermere Supergroup and the early Paleozoic miogeoclinal wedge.

It is important, however, to stress the additional possibility that the older ages proposed for the late Precambrian extensional event are incorrect and that deposition of the Windermere Supergroup occurred much closer to the end of late Precambrian time than has been assumed. The older ages are based on analyses of samples from a single small outcrop of greenstone near the base of the Windermere Supergroup in northeastern Washington (Miller and others, 1973). The analytical results yielded a wide scatter of K-Ar whole-rock ages (233 to 918 Ma), probably because all samples suffered albitization and chloritization during metamorphism subsequent to crystallization. Even the preferred age (827 to 918 Ma) is not tightly constrained. A few other ages that are slightly younger and of uncertain significance have been reported from the southern part of the fold and thrust belt. K-Ar and Rb-Sr ages of 740 to 780 Ma, respectively, were obtained from illite of shales in the Belt-Purcell strata (Goldich and others, 1969), and K-Ar ages of 740 Ma were obtained from muscovite in Belt-Purcell quartzites (Leech, 1962). These data from metasedimentary rocks give only the minimum metamorphic ages and are suspect because the Belt-Purcell deposits were buried deeply beneath the miogeoclinal wedge. Near Cranbrook (Fig. 4), K-Ar ages of 675 and 745 Ma (Leech, 1962) and 675 to 769 Ma (Hunt, 1962) were obtained from a stock and associated intrusions with a Rb-Sr isochron age of 1,260 ± 50 Ma (Ryan and Blenkinsop, 1971). These K-Ar ages also indicate only minimum ages of metamorphism. In the Mackenzie Mountains, Yukon, mafic sills intrusive into strata beneath the Windermere Supergroup have Rb-Sr isochron ages of 769 Ma and 766 Ma, but there is no direct evidence that they are contemporaneous with Windermere deposition (Armstrong and others, 1982).

It should be feasible to distinguish between the possibilities with additional work on the sedimentology and petrology of the Windermere Supergroup and the Hamill Group, and with careful radiometric dating of mafic rocks that occur within these stratigraphic units. Some of the published data about the western part of the southern Canadian Rockies already suggest that a complete passive-margin sequence within the Windermere Supergroup is unlikely. In the Dogtooth Ranges (area II in Fig. 4) and adjacent northern Selkirk Mountains (area I in Fig. 4), rocks assigned to the Windermere Supergroup contain coarse arkosic sediments and mafic volcanics in both the lower and upper parts, suggesting that extensional tectonism occurred through most of the time represented by these strata (Poulton and Simony, 1980; Wheeler, 1963; Brown and others, 1978). In the belt of Windermere strata southwest of the shale basin (Fig. 4), Glover and Price (1977) concluded that the entire upper Precambrian succession is a syntectonic marine-fluvial complex formed by persistent uplift and erosion of a block of the Belt-Purcell Supergroup immediately to the south.

EVIDENCE FOR CRUSTAL THINNING BENEATH THE CARBONATE BANK

In modern passive margins, the continental crust has been significantly modified by crustal thinning over distances of 100 km or more (Keen, 1982; Scrutton, 1982; Grow and Sheridan, 1981), and the thinned crust is separated from normal crust by a zone of variable width, the hinge zone, in which the crustal thickness changes relatively abruptly (Watts, 1981). The thinned crust in modern margins typically is overlain by post-rift sedimentary sequences that are more than about 2 or 3 km thick (Grow and Sheridan, 1981; Keen, 1982), and, by analogy, thinned continental crust could have lain beneath the thick post-rift strata in the outer part

of the carbonate bank (Fig. 6). It is impossible to address this question directly, however, because the miogeoclinal strata have been detached from the basement on which they were deposited and transported more than 100 km eastward onto the craton by the late Mesozoic and early Tertiary thrust faulting (Price, 1980). The entire carbonate-bank facies now lies structurally above Precambrian continental crust that is more than 40 km thick (Price, 1980; Cumming and others, 1979).

The fit between the subsidence curves from the carbonate bank and the model curves with β values greater than one in Figure 8 is not necessarily evidence that the carbonate bank facies was deposited above thinned continental crust. This is the case because the subsidence curves for the various values of β were calculated from a one-dimensional model that assumes a simple Airy type of response of the basement to sediment and water loads. In a simple Airy type of isostatic model, only those points directly beneath the basement loads subside, whereas in a more realistic loading model with flexural compensation, subsidence or flexure of the basement occurs beyond the edges of the load (Watts and others, in press; Watts, 1981). Assuming that the flexural response of basement to loads is similar to loading a thin elastic plate overlying a weak fluid, the basement response function, Φ (equation 1), is (Hetenyi, 1974):

$$\Phi = e^{-\lambda x}(\cos\lambda x + \sin\lambda x) \quad (2)$$

where

$$\lambda = \left[\frac{(\rho_m - \rho_s)g}{4D}\right]^{1/4}; \quad D = \frac{ET_e^3}{12(1-\sigma^2)} \quad (3)$$

λ = flexural parameter, D = flexural rigidity, T_e = elastic thickness, E = Young's modulus, σ = Poisson's ratio, and g = average gravity.

In passive margins, the flexural rigidity, D, increases as heated lithosphere cools and contracts, so that the width of flexural bending, a function of λ in equation 2, increases with time (Watts, 1981; Beaumont and others, 1982). In the context of the passive margin in the southern Canadian Rockies, this means that the sediment and water loads in the shale basin must have deflected or pulled down the basement to the east (Fig. 5) and that a certain amount of the tectonic subsidence in the carbonate bank resulted from the flexural response to loading in the shale basin. Consequently, the β values corresponding to the subsidence curves for the carbonate bank overestimate the amount of stretching (or thinning) of the continental crust that lay beneath the carbonate bank, and the magnitude of the overestimate increases somewhat along the subsidence curves as a function of time.

In modern passive margins, corrections for the effects of flexure are made using two-dimensional thermal and mechanical models of passive margins (Watts, 1981; Beaumont and others, 1982; Steckler and Watts, 1982). This is difficult to attempt in the southern Canadian Rockies, however, because of uncertainties in the original dimensions of the margin and in the thermal and rheological properties of geologically old lithosphere. We have obtained an approximation of upper limit on the magnitude of flexure-controlled subsidence in the carbonate bank, however, by comparing the restored shape of the carbonate bank facies with a hypothetical passive margin in which flexure and lateral heat flow are active. The hypothetical margin was constructed from the two-dimensional extension model of Steckler (1981) that employs finite-element solutions for vertical and lateral heat flow and for flexure caused by both sediment-water loads and the increase in rigidity as heated lithosphere cools and contracts.

In applying this model to the miogeocline, we deliberately overestimated the effect of flexure due to loading in the shale basin by assuming that prior to late Mesozoic–early Tertiary deformation, the shale basin was 240 km wide and the central 80 km was underlain by oceanic crust. The palinspastic increase in width implies a large amount of tectonic shortening in the shale basin, at least by a factor of 3.6, whereas tectonic shortening in the carbonate bank was by a factor of only 2.3 (Price, 1980). It is probable, moreover, that the shale basin was underlain by thinned continental crust rather than oceanic crust (Price, 1980). We also assumed that Te (equation 3), which is the depth to the base of the rheological lithosphere (lithosphere with strength), is at the 550 °C isotherm, an upper value for the observed range of rigidities in oceanic lithosphere (Watts and others, 1980).

The formation of a shale basin, with the dimensions we have assumed, is modeled as a consequence of uniform stretching, with β equal to 1 both at the western edge of the carbonate bank and at the opposite edge of the basin 240 km farther west. The values for β at 40 km and 80 km from the basin edges are equal to 2 and 4, respectively. In the central 80 km of the basin, stretching factors in the crust and mantle are set equal to 6.24 and 9,999, respectively, as required for formation of oceanic lithosphere (Cochran, 1981; Steckler, 1981). The hinge zone is placed at the outer edge of the carbonate bank, so that the tectonic subsidence within the bank will be modeled as due to flexure only.

The results of modeling indicate that the purely flexural response to an overestimate for the magnitude of sediment loading in the shale basin produces a sedimentary wedge that is about 200 km wide with a maximum thickness of 3.2 km at its seaward or western edge (upper part of Fig. 11). This limit is reached after about 100 m.y., approximately the length of time represented by the Lower Cambrian to Middle Ordovician strata that constitute the most complete sections in the carbonate bank. Comparison of the dimensions of this flexural wedge with delithified thicknesses of the Lower Cambrian to Middle Ordovician sedimentary wedge in the northern part of the carbonate bank along A′ (Fig. 1) indicates that there is a significantly greater thickness of strata in the carbonate bank than could have been produced by the overestimate of flexure alone (lower part of Fig. 11). Thermal contraction therefore must have been an important component of the subsidence, at least along the outer edge of the carbonate bank along line A′. The continental crust beneath that part of the carbonate bank must have been thinned during rifting. Because we have overestimated the effect of flexure, it is unlikely that the hinge zone lay farther west than the place at which the maximum thickness of the flexural wedge (3.2 km) matches the restored thicknesses of the Cambrian and Ordovician strata in the carbonate bank. This occurs at approximately the eastward termination of the Lower Cambrian Gog Group (Fig. 6) and, on a nonrestored base, near the Sulphur Mountain Thrust (Fig. 4). By the same reasoning, a probable western limit for the hinge zone farther south is close to columnar section HL7a along B′ and west of ME4b along C′ (Figs. 4, 6).

The inferred westernmost limits for the position of the hinge zone bear an interesting relation to the boundary between the carbonate bank facies and the shale basin. In the north, from A′ to at least as far south as B′, the edge of the carbonate bank lies west of the westernmost limit for the hinge zone, even on a nonrestored base (Fig. 4), and the abrupt transition to the shale facies must be unrelated to mechanisms that operated along the hinge zone. In contrast, a restoration by Price (1980) at the southern end of the shale basin east of Cranbrook (Fig. 4) shows an abrupt increase in thickness of Cambrian and Ordovician strata from 1 km at the western edge of the carbonate bank to more than 4 km in the shale basin a few kilometres to the west. A thickness change of this magnitude clearly is evidence for a rapid transition from craton to a region of tectonic subsidence. The abrupt transition from carbonate to shale facies could have been produced, as Price (1980) suggested, by a rapid increase in subsidence due to abrupt crustal thinning across a hinge zone. The carbonate to shale facies transition, a major lithologic boundary extending for a great distance through the eastern part of the miogeocline, thus appears to have had a complex origin.

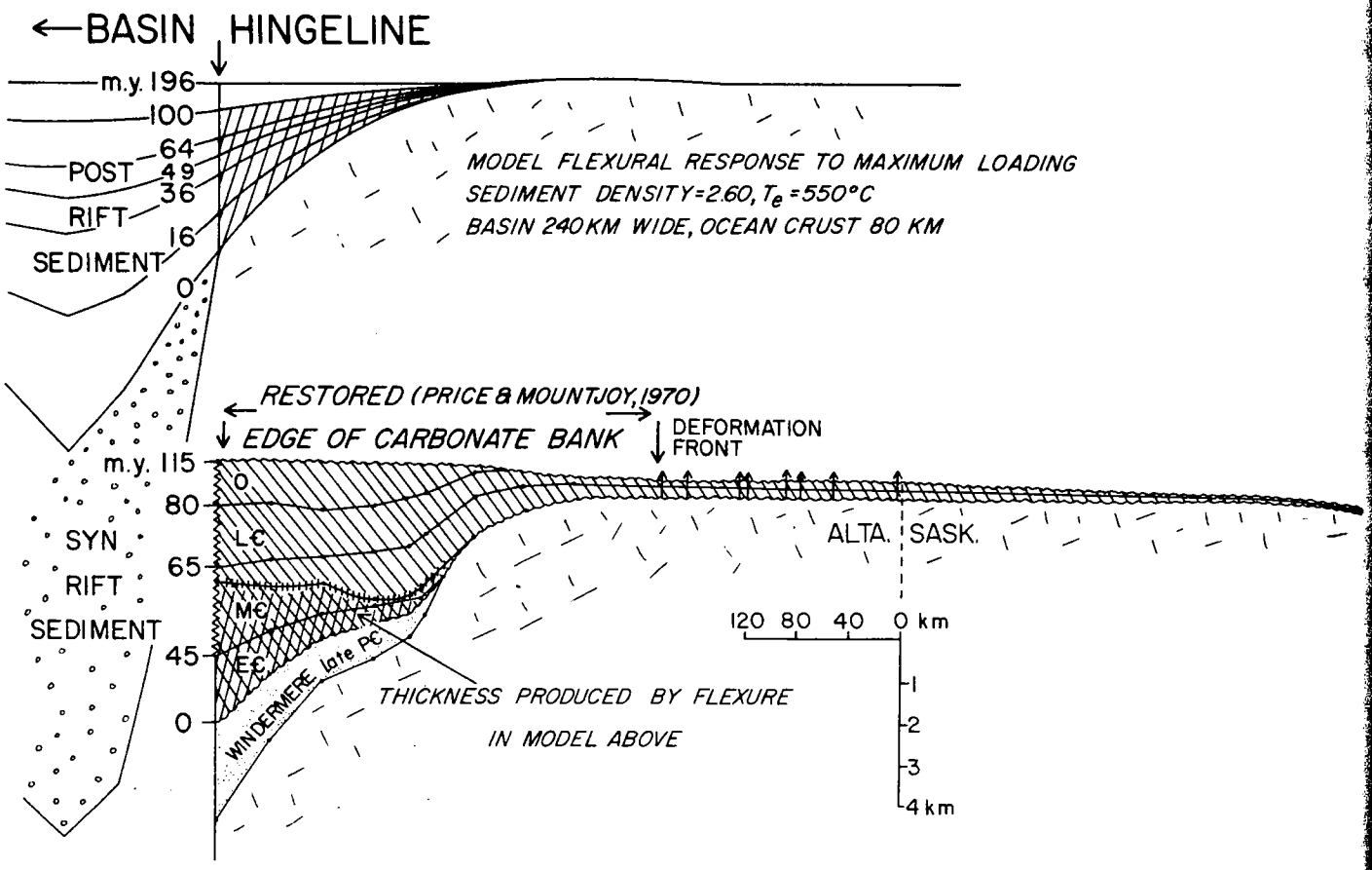

Figure 11. Comparison of a restored cross section of Cambro-Ordovician strata along A′ (in Figs. 4, 6) from the western edge of the carbonate bank to the erosional limit on the craton to the east (lower diagram) with a hypothetical passive margin constructed from a two-dimensional, uniform-stretching model and an overestimate of loading in the shale basin (upper diagram). Inverted Vs indicate locations of wells. Note the much greater thickness of strata in the carbonate bank facies and the greater extent of the Cambrian transgression onto the craton than is predicted by the model for purely flexure-controlled subsidence.

A full understanding of the mechanisms responsible for it remains an important unresolved problem.

Comparison of the hypothetical passive margin with the restores cross section of the inner miogeocline in Figure 11 underscores another problem which concerns the origin of the thin platform sequence that extends eastward onto the craton. This thin sequence extends well beyond the hinge zone of the early Paleozoic margin. Thermal-mechanical modeling of modern passive margins has shown that a significant amount of flexure-controlled subsidence can occur landward of the hinge zone owing to the accumulation of sediment within the margin and the increase in flexural rigidity as the heated lithosphere cools (Keen and others, 1981; Watts, 1981; Steckler and Watts, 1982; Watts, 1982). For a mature margin, the models predict that the sedimentary wedge, or coastal-plain deposit, in the area of subsidence between the hinge zone and the landward limit of deflection can reach a maximum thickness of almost 3.5 km and a width of as much as 200 km (Steckler, 1981; Keen and others, 1981). As the magnitude of the sedimentary load and the rigidity both increase with time, the coastal-plain deposit is a strongly diachronous transgressive wedge that becomes progressively thinner and younger toward the craton. The sedimentary prism produced by flexure in the upper part of Figure 11 is a good example of the wedge shape and diachroneity of a typical coastal-plain deposit, and its dimensions are only slightly smaller than those of the coastal-plain deposit predicted for a mature passive margin.

It is likely that a coastal-plain deposit, possibly of significant size, was present landward of the Cambro-Ordovician hinge zone. In fact, Aitken (1968) showed that the passive-margin wedge in the easternmost part of the thrust and fold belt is diachronous and that Middle to Upper Cambrian formations become younger toward the craton (Fig. 5). Formation of a coastal-plain wedge of any reasonable size and location along the inner edge of the miogeocline, however, clearly could not account for the thin Middle to Upper Cambrian strata that extend for a great distance onto the craton. These strata make up a transgressive deposit that extends to an erosional limit in central Saskatchewan, almost 600 km from the deformation front and more than 800 km from the nonrestored western edge of the carbonate bank (compare upper and lower parts of Fig. 11). There appears to be no obvious tectonic mechanism associated with formation of passive margins that can account

for deposition of a transgressive sheet of such extent. We have suggested previously (Bond and Kominz, 1982) that a eustatic rise of sea level in Middle Cambrian to Early Ordovician time is consistent with the subsidence curves from the carbonate bank and explains the timing and extent of transgression well beyond the limits of flexure-controlled subsidence in the early Paleozoic passive margin. A full discussion of the question of Cambrian and Ordovician eustacy based on our subsidence data and modeling is the subject of a separate paper (Bond and others, in press). It is noteworthy, however, that Vail and others (1977) and Matthews and Cowie (1979) argued that eustacy is the most likely mechanism to explain the apparent synchroneity of Cambrian transgressive deposits on different continents.

SUMMARY AND CONCLUSIONS

A cogent analysis of tectonic subsidence in the miogeocline of the southern Canadian Rocky Mountains is feasible, even though the sequences are deformed and contain diverse, fully lithified strata. Tectonic subsidence curves constructed from stratigraphic columns within the carbonate bank, a linear element along the eastern or inner edge of the miogeocline, have the simple form predicted by models of post-rift thermal contraction in modern passive margins. This result is consistent with the widely held view that the miogeocline is an ancient passive margin and clearly places the Cambrian and Ordovician strata of the carbonate bank in the post-rift or drift phase of the margin. By comparing a restored cross section of the carbonate bank with a hypothetical passive margin constructed from a two-dimensional stretching model, it can be inferred that a hinge zone and thinned continental crust lay beneath the middle to outer part of the carbonate bank. The comparison also implies that the extensive transgressive sheet extending eastward from the miogeocline could not have been deposited in response to processes associated with formation of the early Paleozoic margin, and the transgression could be evidence for a eustatic rise of sea level during Cambrian time.

The tectonic subsidence data from the present studies place much narrower limits on the age at which rifting ended and early Paleozoic thermal subsidence began than has been possible with conventional geologic data. That age, between 555 and 600 Ma, is much younger than previously assumed, and it has significant implications for the history of late Precambrian rifting as well as for the time of breakup and onset of sea-floor spreading. At present, it is not possible to determine whether the age we infer for breakup is the time at which the proto-Pacific ocean began to open or only the time at which a continental fragment broke away from a preexisting proto-Pacific margin. In either case, a latest Precambrian to earliest Cambrian age for continental separation implies a significantly smaller amount of spreading in an ocean basin seaward of the margin than would be implied for breakup closer to the time classically assigned to rifting at 800 to 900 Ma. Moreover, if the continent or continental fragment that was rifted away subsequently collided with another margin, that collision could not have taken place before Early Cambrian time. The young age indicated for breakup also underscores the need for additional field work on two stratigraphic successions in the southern Canadian Rockies: the Windermere Supergroup, which has been regarded as the syn-rift complex, and the overlying Hamill Group, which may contain the evidence for the phase of rifting that led to breakup and the beginning of thermal contraction in the miogeocline.

Detailed studies of well-exposed passive margins, such as in the southern Canadian Rockies, could provide useful data for the ongoing geodynamic studies of passive margins that so far have been focused mainly on modern examples. Because of the large amount of uplift and deep erosion during and following the late Mesozoic and early Tertiary deformation in the Cordilleran miogeocline, complete stratigraphic sequences from the syn-rift through the post-rift stages of the early Paleozoic margin are well exposed throughout the Cordillera. This allows direct observation of stratigraphic intervals the counterparts of which in modern passive margins are poorly known owing to deep burial. For example, the transition from the rifting to drift stage, which typically lies at depths of a few kilometres in modern margins, is poorly understood; yet, large hydrocarbon reserves, such as in the Hibernia area (Arthur and others, 1982), have been discovered within the sequences deposited near the transition. Limited data from some modern margins suggest that the transition does not develop as predicted by the simple stretching model of McKenzie (1978), especially where an unconformity (the breakup unconformity) separates the syn-rift and post-rift strata (Royden and Keen, 1980). In the southern Canadian Rockies, and probably elsewhere in the Cordillera, the strata deposited during the rift-drift transition are well exposed and, in the southern Canadian Rockies, the widespread sub-Cambrian unconformity (Fig. 5) could be analogous to the breakup unconformity of modern margins. Detailed studies of strata spanning the rift-drift transition in the miogeocline could be undertaken for comparison with various passive margin models and to develop depositional models for this important phase in passive margin evolution.

ACKNOWLEDGMENTS

We thank Ray Price, Jim Aitken, Andrew Okulitch, and Mike Cecile of the Geological Survey of Canada; Walter Pitman, Tony Watts, and Jim Cochran of Lamont-Doherty Geological Observatory; and Bill Dickinson for critical reviews of earlier versions of this manuscript and advice at various stages of field work. Research was supported by National Science Foundation Grant OCE 79 26308 to A. B. Watts and W. Pitman; by grants from Shell Exploration in Calgary, Shell Research and Development in Houston, and the Arco Research Foundation; and, in the later stages of the project, by National Science Foundation Grant EAR 82-12737 to G. Bond and H. Brueckner.

APPENDIX 1: CALCULATION OF TECTONIC SUBSIDENCE

To calculate the tectonic subsidence, Y, of equation 1, we replaced S^* with D_n, the thickness of the entire sediment column at the time of deposition of the n^{th} lithologic unit, and we replaced ρ_s (equation 1) with ρ_{sn}, the bulk density of the sediment column at the time of deposition of the n^{th} lithologic unit:

$$D_n = \frac{D_{mn} + D_{cn}}{2} \pm \frac{D_{mn} - D_{cn}}{2} \qquad \text{(A-1)}$$

and

$$\rho_{sn} = \frac{\rho_{mn} + \rho_{cn}}{2} \pm \frac{\rho_{mn} - \rho_{cn}}{2}, \qquad \text{(A-2)}$$

where m designates porosity loss due only to compaction and c designates porosity loss due to precipitation of cement in all lithologies except shale. The derivation of D_{mn}, D_{cn}, ρ_{mn}, and ρ_{cn} has the form of:

$$D_{xn} = \sum_{j=1}^{n} O_j K_{xj} \qquad \text{(A-3)}$$

and

$$\rho_{xn} = \frac{1}{D_{xn}} \sum_{j=1}^{n} O_j \rho_j K_{xj}, \qquad \text{(A-4)}$$

where x is either the m or c option for porosity loss, ρ_j = bulk density of sediment in j^{th} lithologic unit, O_j = observed, fully compacted sediment thickness in j^{th} lithologic unit, and K_{xj} = thickness correction for the j^{th} lithologic unit. The bulk density of each lithologic unit j is calculated from:

$$\rho_j = \sum_{j=1}^{6} F_{ij} \left\{ \rho_{gi} (1 - \phi_{ij}) + \rho_w \phi_{ij} \right\}, \quad \text{(A-5)}$$

where i = i^{th} lithology, of which there are six in the Canadian miogeocline; ρ_{gi} = the grain density of the i^{th} lithology; ρ_w = the density of sea water; F_{ij} = the proportion of lithology i in the j^{th} lithologic unit; and ϕ_{ij} = the average porosity of the i^{th} lithology in the j^{th} lithologic unit from equation A-8. The thickness correction, K_x, for mechanical compaction is:

$$K_{mj} = 1 + \sum_{i=1}^{6} F_{ij} \left(\frac{1}{1 - \phi_{ij}} \right) - 1 \quad \text{(A-6)}$$

and for cementation is:

$$K_{cj} = 1 + F_{shj} \left(\frac{1}{1 - \phi_{shj}} \right) - 1 \quad , \quad \text{(A-7)}$$

where F_{ij} = the proportion of the i^{th} lithology in the j^{th} unit, F_{shj} = the proportion of shale in the j^{th} unit, and the mean porosity of the i^{th} lithology in the j^{th} unit is defined by:

$$\phi_{ij} = \frac{1}{z_2 - z_1} \left[\int_{z_{ai}}^{z_2} \phi_{Ai} \exp(-z k_{Ai}) dz + \int_{z_1}^{z_{ai}} \phi_{Bi} \exp(-z k_{Bi}) \right] , \quad \text{(A-8)}$$

and ϕ_i, the porosity of lithology i, is defined over two intervals as:

$$\phi_i = \begin{cases} \phi_{Ai} \exp(-z k_{Ai}) & ; (z_{ai} < z < \infty) \\ \phi_{Bi} \exp(-z k_{Bi}) & ; (z_{ai} > z > 0) \end{cases} , \quad \text{(A-9)}$$

where i = one of six specified lithologies (shale—sh in equation A-7, micrite, quartz sandstone, calcarenite, siltstone, and calcisiltstone), ϕ_{Ai} and ϕ_{Bi} are porosities at 0 depth for the i^{th} lithology, k_{Ai} and k_{Bi} are exponential decay constants for i^{th} lithology, z = depth at which ϕ_i is calculated from Figure 2, and z_{ai} = depth at change of slope for porosity versus depth in Figure 2.

REFERENCES CITED

Aitken, J. D., 1966, Middle Cambrian to Middle Ordovician cyclic sedimentation, southern Rocky Mountains of Alberta: Bulletin of Canadian Petroleum Geology, v. 14, p. 405-441.

——— 1968, Cambrian sections in the easternmost southern Rocky Mountains and the adjacent subsurface, Alberta: Geological Survey of Canada Paper 66-23.

1971, Control of lower Paleozoic sedimentary facies by the Kicking Horse Rim, southern Rocky Mountains, Canada: Bulletin of Canadian Petroleum Geology, v. 19, p. 557-569.

1978, Revised models for depositional grand cycles, Cambrian of the southern Rocky Mountains, Canada: Bulletin of Canadian Petroleum Geology, v. 26, p. 515-542.

Aitken, J. D., and Gregg, R. G., 1967, Upper Cambrian formations, southern Rocky Mountains of Alberta, an interim report: Geological Survey of Canada Paper 66-79, 91 p.

Aitken, J. D., and Norford, B. S., 1967, Lower Ordovician Survey Peak and Outram Formations, southern Rocky Mountains of Alberta: Bulletin of Canadian Petroleum Geology, v. 15, p. 150-207.

Aitken, J. D., Fritz, W. H., and Norford, B. S., 1972, Cambrian and Ordovician biostratigraphy of the southern Canadian Rocky Mountains: International Geological Congress, 24th, Montreal, Guidebook, Field Excursion A19, 57 p.

Armstrong, R. L., 1978, Pre-Cenozoic Phanerozoic time scale: Computer file of critical dates and consequences of new and in progress decay-constant revisions, *in* Cohee, G. V., Glassner, M. F., and Hedberg, H. D., eds., Contributions to the geologic time scale: American Association of Petroleum Geologists Studies in Geology, No. 6, p. 73-91.

Armstrong, R. L., Eisbacher, G. H., and Evans, P. D., 1982, Age and stratigraphic-tectonic significance of Proterozoic diabase sheets, Mackenzie Mountains, northwestern Canada: Canadian Journal of Earth Sciences, v. 19, p. 316-323.

Arthur, K. R., Cole, D. R., Henderson, G.G.L., and Kushnir, D. W., 1982, Geology of the Hibernia discovery, *in* Halbouty, M.T., ed., The delicate search for the subtle trap: American Association of Petroleum Geologists Memoir 32, p. 181-197.

Bathurst, R.G.C., 1976, Carbonate sediments and their diagenesis: Developments in sedimentology 12: Amsterdam, Elsevier, 658 p.

Beales, F., 1971, Cementation in ancient pelleted limestones, *in* Bricker, O. P., ed., Carbonate cements: Baltimore, Maryland, Johns Hopkins University Press, p. 216-224.

Beard, D. C., and Wyel, P. K., 1973, Influence of texture on porosity and permeability of unconsolidated sand: American Association of Petroleum Geologists Bulletin, v. 57, p. 349-369.

Beaumont, C., Keen, C. E., and Boutilier, R., 1982, On the evolution of rifted continental margins: Comparison of models and observations for the Nova Scotian Margin: Royal Astronomical Society Geophysical Journal, v. 70, p. 667-715.

Benvenuto, G. L., and Price, R. A., 1979, Structural evolution of the Hosmer Thrust Sheet, southeastern British Columbia: Bulletin of Canadian Petroleum Geology, v. 27, p. 360-394.

Birkelund, T., Bridgewater, D., Higgins, A. K., and Perch-Nielsen, K., 1974, An outline of the geology of the Atlantic coast of Greenland, *in* Nairn, A.E.M., and Stehli, F. G., eds., The ocean basins and their margins—2, The North Atlantic: New York, Plenum, p. 125-160.

Blatt, H., 1979, Diagenetic processes in sandstones, *in* Scholle, P. A., and Schluger, P. R., eds., Aspects of diagenesis: Society of Economic Paleontologists and Mineralogists Special Publication 26, p. 141-157.

Bond, G. C., and Kominz, M. A., 1981, The problem of subsidence mechanisms for the lower Paleozoic stratigraphic succession in the southern Canadian Rocky Mountains: Geological Society of America Abstracts with Programs, v. 13, p. 191.

——— 1982, Evidence for thermal subsidence and eustatic sea level change from the lower Paleozoic miogeocline in western North America: Geological Society of America Abstracts with Programs, v. 14, p. 447.

Bond, G. C., Kominz, M. A., and Devlin, W. J., in press, Thermal subsidence and eustacy in the lower Paleozoic miogeocline of western North America: Nature.

Brown, R. L., Tippett, C. R., and Lane, L. S., 1978, Stratigraphy, facies changes, and correlations in the northern Selkirk Mountains, southern Canadian Cordillera: Canadian Journal of Earth Sciences, v. 15, p. 1129-1140.

Burchfiel, B. C., and Davis, G. A., 1972, Structural framework and evolution of the southern part of the Cordilleran orogen, western United States: American Journal of Science, v. 272, p. 97-118.

——— 1975, Nature and controls of Cordilleran orogenesis, western United States: Extensions of an earlier synthesis: American Journal of Science, v. 275A, p. 363-396.

Burke, K., 1976, Development of graben associated with the initial ruptures of the Atlantic Ocean: Tectonophysics, v. 36, p. 93-112.

Chilingarian, G. V., and Wolf, K. H., 1975, Compaction of coarse-grained sediments, I: Amsterdam, Elsevier, 552 p.

——— 1976, Compaction of coarse-grained sediments, II: Amsterdam, Elsevier, 808 p.

Choquette, P. W., and Pray, L. C., 1970, Geologic nomenclature and classification of porosity in sedimentary carbonates: American Association of Petroleum Geologists Bulletin, v. 54, p. 207-250.

Christiansen, T. B., Schaefer, H.-U., and Schonfeld, M., 1975, Southern Afar and adjacent areas: Geology, petrology, geochemistry, *in* Pilger, A., and Rosler, A., eds., Afar Depression of Ethiopia: Inter-Union Commission on Geodynamics Scientific Report 14, E. Schweizerbart'sche Verlagsbuchhandlung, Stuttgart, p. 259-277.

Cochran, J. R., 1981, Simple models of diffuse extension and the pre-seafloor spreading development of the continental margin of the northeastern Gulf of Aden, *in* Blanchet, R., and Montadert, L., Geology of continental margins: International Geological Congress, 26th, Proceedings: Oceanologica Acta, p. 155-165.

Coney, P. J., Jones, D. L., and Monger, J.W.H., 1980, Cordilleran suspect terranes: Nature, v. 288, p. 329-333.

Coogan, A. J., 1970, Measurements of compaction in oolitic grainstone: Journal of Sedimentary Petrology, v. 40, p. 921-929.

Cook, D. G., 1970, A Cambrian facies change and its effect on structure, Mount Stephen-Mount Dennis area, Alberta: British Columbia and Wheeler, J. O., ed., Structure of the southern Canadian Cordillera: Geological Association of Canada Special Paper 6, p. 27-39.

1975, Structural style influenced by lithofacies, Rocky Mountain Main Ranges, Alberta: British Columbia: Geological Survey of Canada Bulletin 288, 73 p.

Cowie, J. W., and Cribb, S. J., 1978, The Cambrian system, *in* Cohee, G. V., Glaessner, M. F., and Hedberg, H. D., eds., The geologic time scale: American Association of Petroleum Geologists, Studies in Geology, No. 6, p. 355-362.

Cowie, J. W., Rushton, A. W. A., and Stubblefield, C. J., 1971, A correlation of Cambrian rocks in the British Isles: Geological Society of London, Special Report 2, 42 p.

Cumming, W. B., Glowes, R. M., and Ellis, R. M., 1979, Crustal structure from a seismic refraction profile across southern British Columbia: Canadian Journal of Earth Sciences, v. 16, p. 1024-1040.

Daly, R. D., Manger, G. E., and Clark, S. P., Jr., 1966, Density of rocks, *in* Clark, S. P., Jr., ed., Handbook of physical constants: Geological Society of America Memoir 97, p. 19-26.

de Charpal, O., Guennoc, P., Montadert, L., and Roberts, D. G., 1978, Rifting, crustal attenuation and subsidence in the Bay of Biscay: Nature, v. 275, p. 706-711.

Dewey, J. F., and Burke, K., 1974, Hotspots and continental breakup: Implications for collisional orogeny: Geology, v. 2, p. 57-60.

Dickinson, W. R., 1977, Plate tectonics and sedimentation, *in* Dickinson, W. R., ed., Tectonics and sedimentation: Society of Economic Paleontologists and Mineralogists Special Publication 22, p. 1-28.

Ellison, A. H., 1967, The Hamill Group of the northern Dogtooth Mountains, British Columbia, Canada [M.Sc. thesis]: Calgary, Canada, University of Calgary, Department of Geology.

Enos, P., and Sawatsky, L. H., 1980, Pore networks in Holocene carbonate sediments: Journal of Sedimentary Petrology, v. 51, p. 961-985.

Fitch, F. J., Forster, S. C., and Miller, J. A., 1976, The dating of the Ordovician, *in* Bassett, M. G., ed., The Ordovician system: Palaeontological Association Symposium, University of Wales Press, Cardiff.

Friedman, G. M., 1975, The making and unmaking of limestones or the downs and ups of porosity: Journal of Sedimentary Petrology, v. 45, p. 379-398.

Fuchtbauer, H., 1974, Sediments and sedimentary rocks, Part II: New York, Halsted Press, 464 p.

Fyles, J. T., and Eastwood, G.E.P., 1962, Geology of the Ferguson area, Lardeau District, British Columbia: British Columbia Department of Mines and Petroleum Resources Bulletin 45.

Gabrielse, H., 1972, Younger Precambrian of the Canadian Cordillera: American Journal of Science, v. 272, p. 521-536.

Gale, N. H., Beckinsale, R. D., and Wadge, A. J., 1979, A Rb-Sr whole rock isochron for the stockdale rhyolite of the English Lake District and a revised mid-Paleozoic time scale: Journal of the Geological Society of London, v. 136, p. 235-242.

——— 1980, Discussion of a paper by McKerrow, Lambert and Chamberlain on the Ordovician, Silurian and Devonian time scales: Earth and Planetary Science Letters, v. 57, p. 9-17.

Glover, J. K., and Price, R. A., 1977, Stratigraphy and structure of the Windermere Supergroup, southern Kootenay Arc, British Columbia: Geological Survey of Canada Paper 76-1B, p. 21-23.

Goldich, S. S., Baadsgaard, H., Edwards, G., and Weaver, C. E., 1969, Investigations in radioactivity-dating of sediments: American Association of Petroleum Geologists Bulletin, v. 43, p. 654-662.

Grow, J. A., and Sheridan, R. E., 1981, Structure and evolution of the U.S. Atlantic continental margin, *in* Blanchet, R., and Montadert, L., eds., Geology of continental margins: International Geological Congress, 26th, Paris, Proceedings: Oceanologica Acta, v. 4, p. 11-21.

Halley, R. B., 1979, Petrographic summary, *in* Scholle, P. A., ed., Geological studies of the COST GE-1 well, United States South Atlantic outer continental shelf area: U.S. Geological Survey Circular 800, p. 42-49.

Hardenbol, J., Vail, P. R., and Ferrer, J., 1981, Interpreting paleoenvironments, subsidence history and sea level changes of passive margins from seismic and biostratigraphy, *in* Blanchet, R., and Montadert, L., eds., Geology of continental margins: International Geological Congress, 26th, Proceedings: Oceanologica Acta, p. 33-44.

Harland, W. B., and Francis, E. H., eds., 1971, The Phanerozoic time-scale—A supplement: Geological Society of London Special Publication 5, p. 1-120.

Harland, W. B., Cox, A. V., Llewellyn, P. G., Picton, C.A.G., Smith, A. G., and Walters, R., 1982, A geologic time scale: Cambridge, Cambridge University Press.

Harrison, J. E., and Reynolds, M. W., 1976, Western U.S. continental margin: A stable platform dominated by vertical tectonics in the late Precambrian: Geological Society of America Abstracts with Programs, v. 8, p. 905.

Heteny, M., 1974, Beams on elastic foundation: Ann Arbor, Michigan, University of Michigan Press, 255 p.

Höy, T., 1977, Stratigraphy and structure of the Kootenay Arc in the Riondel area, southeastern British Columbia: Canadian Journal of Earth Sciences, v. 14, p. 2301-2315.

——— 1979, Geology of the Goldstream area: British Columbia Department of Energy, Mines and Petroleum Resources Bulletin 71, 63 p.

Hunt, G., 1962, Time of Purcell eruption in southeastern British Columbia and southwestern Alberta: Alberta Society of Petroleum Geologists Journal, v. 10, p. 438-442.

Jarvis, G. T., and McKenzie, D. P., 1980, Sedimentary basin formation with finite extension rates: Earth and Planetary Science Letters, v. 48, p. 42-52.

Kanasewich, E. R., Clawes, R. M., and McCloughan, C. H., 1969, A buried Precambrian rift in western Canada: Tectonophysics, v. 8, p. 513-52

Lorenz, C. D., and Watts, A. B., 1982, On isostasy at Atlantic-type continental margins: Journal of Geophysical Research, v. 87, p. 2923-2948.

Bass, C. E., 1979, Thermal history and subsidence of rifted continental margins: Evidence from wells on the Nova Scotian and Labrador shelves: Canadian Journal of Earth Sciences, v. 15, p. 505-522.
1982, The continental margins of eastern Canada: review, *in* Scrutton, R. A., ed., Dynamics of passive margins: Geodynamics Series, v. 6, p. 45-58.

Bott, C. F., Beaumont, C., and Boutilier, R., 1981, Preliminary results from a thermo-mechanical model for the evolution of Atlantic-type continental margins: *in* Blanchert, R., International Geological Congress, 26th, Proceedings: Oceanologica Acta, p. 123-128.

Bowsher, M. A., and Bond, G. C., 1982, Tectonic subsidence calculated from lithified basin strata: Geological Society of America Abstracts with Programs, v. 14, p. 534.

Lowdon, E. Taylor, M. E., and Erdtmann, B. D., 1978, Correlation of the Cambrian-Ordovician boundary between the Acado-Baltic and North American faunal provinces: Geology, v. 6, p. 75-78.

Leech, G. B., 1962, Metamorphism and granitic intrusions of Precambrian age in southeastern British Columbia: Geological Survey of Canada Paper 62-13, 8 p.
——— 1965, Kananaskis (west half) map area: Report of activities: Geological Survey of Canada Paper 65-1, p. 77.

Eisbacher, G. H., and Price, R. A., 1976, Large-scale block faulting during deposition in the Windermere Supergroup (Hadrynian) in southeastern British Columbia: Geological Survey of Canada Paper 76-1A, p. 135-136.

Bjorlykke, K., 1980, Comparison of porosity-depth relationships of shale and sandstone: Journal of Petroleum Geology, v. 3, p. 175-185.

Matthews, S. C., and Cowie, J. W., 1979, Early Cambrian transgressions: Geological Society of London Journal, v. 136, p. 133-135.

Maxwell, J. C., 1964, Influence of depth, temperature and geologic age on porosity of quartzose sandstone: American Association of Petroleum Geologists Bulletin, v. 48, p. 697-769.

Mudge, M. R., and Yates, R. A., 1974, Stratigraphic relationships at the western edge of the Middle Cambrian carbonate facies belt, Field, British Columbia: Geological Survey of Canada Paper 74-1, Part A, p. 333-334.

Nelson, D., 1978, Some remarks on the development of sedimentary basins: Earth and Planetary Science Letters, v. 40, p. 25-32.

Norford, B. S., Lambert, R. St. J., and Chamberlain, V. E., 1980, The Ordovician, Silurian and Devonian time scales: Earth and Planetary Science Letters, v. 51, p. 1-8.

Parrish, M. F., and Price, R. A., 1982, Superimposed low-grade metamorphism in the Mount Fisher area, southeastern British Columbia—Implications for the east Kootenay orogeny: Canadian Journal of Earth Sciences, v. 19, p. 476-489.

Price, R. A., McKee, E. H., and Yates, R. G., 1973, Age and correlation of the Windermere Group in northeastern Washington: Geological Society of America Bulletin, v. 84, p. 3723-3730.

Price, R. A., and Price, R. A., 1979, Geodynamic evolution of the Canadian Cordillera—Progress and problems: Canadian Journal of Earth Sciences, v. 16, p. 770-791.

Rutford, R. S., 1969, Ordovician and Silurian stratigraphy of the southern Rocky Mountains: Geological Survey of Canada Bulletin 176, 90 p.

Schiarizza, A. V., 1974, Stratigraphy and structure of the Mount Ida Group, Vernon (82L), Seymour Arm (82M), Bonaparte Lake (92P) and Kettle River (82E) map-areas, British Columbia: Geological Survey of Canada Paper 74-1, Part A, p. 25-30.
1975, Stratigraphy and structure of the western margin of the Shuswap metamorphic complex, Vernon (82L) and Seymour Arm (82M) map areas, British Columbia: Geological Survey of Canada Paper 75-1, Part A, p. 27-28.

Silverwatch, N. C., 1967, Geology of Wildcat Hills (west half), Alberta: Geological Survey of Canada Map 1351A.

Parsons, B., and Sclater, J. G., 1977, Analysis of the variation of ocean floor bathymetry and heat flow with age: Journal of Geophysical Research, v. 82, p. 803-827.

Perrier, R., and Quiblier, J., 1974, Thickness changes in sedimentary layers during compaction history: methods for quantitative evaluation: American Association of Petroleum Geologists Bulletin, v. 58, p. 507-520.

Poulton, T. P., and Simony, P. S., 1980, Stratigraphy, sedimentology, and regional correlation of the Horsethief Creek Group (Hadrynian, late Precambrian) in the northern Purcell and Selkirk Mountains, British Columbia: Canadian Journal of Earth Sciences, v. 17, p. 1708-1724.

Price, R. A., 1980, The Cordilleran foreland thrust and fold belt in the southern Canadian Rocky Mountains: Geological Society of London Special Publication 9, p. 1-22.

Price, R. A., and Mountjoy, E. W., 1970, Geologic structure of the Canadian Rocky Mountains between Bow and Athabasca Rivers—A progress report, *in* Wheeler, J. O., ed., Structure of the southern Canadian Cordillera: Geological Association of Canada Special Paper 6, p. 7-25.
——— 1971, Geology, Lake Minnewanka (west half), Alberta: Geological Survey of Canada Map 1272A.
——— 1972a, Geology, Banff (east half), Alberta: British Columbia Geological Survey of Canada Map 1295A.
——— 1972b, Geology, Banff (east Half), Alberta: Geological Survey of Canada Map 1295A.
——— 1972c, Geology, Mount Eisenhower (east half), Alberta: Geological Survey of Canada Map 1296A.
——— 1972d, Geology, Mount Eisenhower (west half), Alberta: Geological Survey of Canada Map 1297A.
——— 1978a, Geology, Hector Lake (east half), Alberta: British Columbia Geological Survey of Canada Map 1463A.
——— 1978b, Geology, Hector Lake (west half), Alberta: British Columbia Geological Survey of Canada Map 1464A.
——— 1978c, Geology, Siffleur River (east half), Alberta: Geological Survey of Canada Map 1465A.
——— 1978d, Geology, Siffleur River (west half), Alberta: Geological Survey of Canada Map 1466A.

Price, R. A., and Ollerenshaw, N. C., 1971a, Geology of Scalp Creek (west half), Alberta: Geological Survey of Canada Map 1276A.
——— 1971b, Geology of Scalp Creek (east half), Alberta: Geological Survey of Canada Map 1275A.

Read, P. B., 1973, Petrology and structure of the Poplar Creek map-area, British Columbia: Geological Survey of Canada Bulletin 193, 144 p.
——— 1975, Lardeau Group, Lardeau map area, west half, British Columbia: Geological Survey of Canada Paper 75-1, Part A, p. 28.

Reesor, J. E., 1973, Geology of the Lardeau map-area (east half), British Columbia: Geological Survey of Canada Memoir 369, 129 p.

Rieke, H. H., III, and Chilingarian, G. V., 1974, Compaction of argillaceous sediments: Amsterdam, Elsevier, 424 p.

Robinson, R. A., Rosova, A. V., Rowell, A. J., and Fletcher, T. P., 1977, Cambrian boundaries and divisions: Lethaia, v. 10, p. 257-262.

Ross, J. V., 1970, Structural evolution of the Kootenay Arc, southeastern British Columbia, *in* Wheeler, J. O., ed., Structure of the southern Canadian Cordillera: Geological Association of Canada Special Paper 6, p. 53-65.

Royden, L., and Keen, C. E., 1980, Rifting process and thermal evolution of the continental margin of eastern Canada determined from subsidence curves: Earth and Planetary Science Letters, v. 51, p. 343-361.

Royden, L., Sclater, J. G., and Von Herzen, R. P., 1980, Continental margin subsidence and heat flow: Important parameters in formation of petroleum hydrocarbons: American Association of Petroleum Geologists Bulletin, v. 64, p. 173-187.

Ryan, B. C., and Blenkinsop, J., 1971, Geology and geochronology of the Hellroaring Creek Stock, British Columbia: Canadian Journal of Earth Sciences, v. 8, p. 85-95.

Schmidt, V., and McDonald, D. A., 1979, Texture and recognition of secondary porosity in sandstones, *in* Scholle, P. A., and Schlager, P. R., eds., Aspects of diagenesis: Society of Economic Paleontologists and Mineralogists Special Publication 26, p. 209-226.

Schmoker, J. W., and Halley, R. B., 1982, Carbonate porosity versus depth: A predictable relation for south Florida: American Association of Petroleum Geologists Bulletin, v. 66, p. 2561-2570.

Scholle, P. A., 1977, Chalk diagenesis and its relation to petroleum exploration: Oil from chalks, a modern miracle?: American Association of Petroleum Geologists Bulletin, v. 61, p. 982-1009.

Sclater, J. G., and Christie, P.A.F., 1980, Continental stretching: An explanation of the post-mid-Cretaceous subsidence of the central North Sea basin: Journal of Geophysical Research, v. 85, p. 3711-3739.

Scrutton, R. A., ed., 1982, Dynamics of passive margins: Geodynamics Series, Volume 6: Washington, D.C., American Geophysical Union, 200 p.

Sears, J. S., and Price, R. A., 1978, The Siberian connection: A case for Precambrian separation of the North American and Siberian Cratons: Geology, v. 6, p. 267-270.

Shinn, E. A., 1969, Submarine lithification of Holocene carbonate sediments in the Persian Gulf: Sedimentology, v. 12, p. 109-144.

Shinn, E. A., Halley, R. B., Hudson, J. H., and Lidz, B. H., 1977, Limestone compaction: An enigma: Geology, v. 5, p. 21-24.

Simony, P. S., and Wind, G., 1970, Structure of the Dogtooth Range and adjacent portions of the Rocky Mountain Trench, *in* Wheeler, J. O., ed., Structure of the southern Canadian Cordillera: Geological Association of Canada Special Paper No. 6, p. 41-51.

Sleep, N. H., 1971, Thermal effects of the formation of Atlantic continental margins by continental breakup: Royal Astronomical Society Geophysical Journal, v. 24, p. 325-350.

Steckler, M. S., 1981, Thermal and mechanical evolution of Atlantic-type margins [Ph.D. thesis]: New York, Columbia University, 261 p.

Steckler, M. S., and Watts, A. B., 1978, Subsidence of the Atlantic-type continental margins off New York: Earth and Planetary Science Letters, v. 41, p. 1-13.
——— 1982, Subsidence history and tectonic evolution of Atlantic-type continental margins, *in* Scrutton, R. A., ed., Dynamics of passive margins, Geodynamics Series, Volume 6, Washington, D.C., American Geophysical Union, p. 184-196.

Stewart, J. H., 1971, Late Precambrian (~750 m.y.) continental separation in western North America—Possible evidence from sedimentary and volcanic rocks: Geological Society of America Abstracts with Programs, v. 3, no. 2, p. 201.
——— 1972, Initial deposits in the Cordilleran geosyncline: Evidence of a late Precambrian (~850 m.y.) continental separation: Geological Society of America Bulletin, v. 83, p. 1345-1360.
——— 1976, Late Precambrian evolution of North America: Plate tectonics implication: Geology, v. 4, p. 11-15.

Stewart, J. H., and Suczek, C. A., 1977, Cambrian and latest Precambrian paleogeography and tectonics in the western United States, *in* Stewart, J. H., Stevens, C. H., and Fritsche, A. E., Paleozoic paleogeography of the western United States: Society of Economic Paleontologists and Mineralogists, Pacific Section, Pacific Coast Paleogeography Symposium 1, p. 1-17.

Sweet, W. C., and Bergstrom, S. M., 1976, Conodont biostratigraphy of the Middle and Upper Ordovician of the United States midcontinent, *in* Bassett, M. G., The Ordovician system: Proceedings of a paleontological association symposium, Birmingham: Cardiff, Wales, University of Wales Press, p. 121-151.

Vail, P. K., Mitchum, R. M., Jr., and Thompson, S., III, 1977, Seismic stratigraphy and global changes of sea level—Part 4, Global cycles of relative changes of sea level, *in* Payton, E. D., ed., Seismic stratigraphy—Applications to hydrocarbon exploration: Tulsa, Oklahoma, American Association of Petroleum Geologists Memoir 26, p. 83-97.

Van Hinte, J. E., 1978, Geohistory analysis—Applications of micropaleontology in exploration geology: American Association of Petroleum Geologists Bulletin, v. 62, p. 201-222.

Veevers, J. J., and Cotterill, D., 1978, Western margin of Australia: Evolution of a rifted arch system: Geological Society of America Bulletin, v. 89, p. 337-355.

Von Engelhardt, W., 1973, Die Bildung von sedimenten und Sedimentgesteinen, Sediment-Petrologie, Teil III: Stuttgart, E. Schneizerbart'sche, 378 p.

Watts, A. B., 1981, The U.S. Atlantic continental margin: Subsidence history, crustal structural and thermal evolution, *in* Geology of passive continental margins: History, structure and sedimentologic record: American Association of Petroleum Geologists Continuing Education Course Note Series no. 19, chap. 2, 75 p.
——— 1982, Tectonic subsidence, flexure and global changes of sea level: Nature, v. 297, p. 469-474.

Watts, A. B., and Ryan, W.B.F., 1976, Flexure of the lithosphere and continental margin basins: Tectonophysics, v. 36, p. 24-44.

Watts, A. B., and Steckler, M. S., 1979, Subsidence and eustacy at the continental margin of eastern North America: Maurice Ewing Series, Volume 3: Washington D.C., American Geophysical Union, p. 218-234.

Watts, A. B., Bodine, J. H., and Ribe, N. M., 1980, Observations of flexure and the geological evolution of the Pacific Ocean basin: Nature, v. 283, p. 432-537.

Watts, A. B., Karner, G. D., and Steckler, M. S., in press, Crustal flexure and the driving mechanism of sedimentary basin formation: Royal Society of London Proceedings.

Wheeler, J. O., 1963, Rogers Pass map-area, British Columbia and Alberta: Geological Survey of Canada Paper 62-32, 32 p.

Williams, A., 1976, Plate tectonics and biofacies evolution as factors in Ordovician correlations, *in* Bavelt, M. G., The Ordovician system: Proceedings of a paleontological association symposium, Birmingham: Cardiff, Wales, University of Wales Press, p. 29-66.

Young, G. M., Jefferson, C. W., Delaney, G. D., and Yeo, G. M., 1979, Middle and late Proterozoic evolution of the northern Canadian Cordillera and shield: Geology, v. 7, p. 125-128.

Zankl, H., 1969, Structural and textural evidence of early lithification in fine-grained carbonate rocks: Sedimentology, v. 12, p. 241-256.

MANUSCRIPT RECEIVED BY THE SOCIETY JULY 6, 1982
REVISED MANUSCRIPT RECEIVED APRIL 2, 1983
MANUSCRIPT ACCEPTED APRIL 7, 1983
LAMONT-DOHERTY GEOLOGICAL OBSERVATORY CONTRIBUTION NO. 3565

Printed in U.S.A.